Functional Investigation of Histone Demethylation on Skin Stem Cell Proliferation and Differentiation

By:

Sarah Cayee Ha

Dept. of Molecular, Cellular, and Developmental Biology

University of Colorado at Boulder

Defense Date:

April 3, 2013

Thesis Advisor:

Dr. Rui Yi, Dept. of Molecular, Cellular and Developmental Biology

Defense Committee:

Dr. Rui Yi, Dept. of Molecular, Cellular and Developmental Biology

Dr. Johannes Rudolph, Dept. of Chemistry and Biochemistry

Sally Green, Program for Writing and Rhetoric

Abstract

Histone demethylases are proteins that remove methyl groups on lysine or arginine residues on histone core proteins in the nucleus. Through the demethylation of histone proteins, these enzymes play an essential role in the regulation of many biological processes. Although histone demethylases have been associated with regulatory pathways, their functionality is still largely unknown. To investigate the functional role of histone demethylation in regulatory pathways such as proliferation and differentiation in skin stem cells, I employed a small molecule, Methylstat, to competitively inhibit histone demethylases. In my thesis study, I cultured isolated murine epidermal skin stem cells and human squamous cell carcinoma (SCC) cells to observe and analyze the dynamics of self-renewal and terminal differentiation imbued with different concentrations of Methylstat to induce a global inhibition of histone demethylases. By treating skin cells, or keratinocytes, with Methylstat, I demonstrated that histone demethylation inhibition caused a decrease in proliferation and induced premature cell death. Additionally, I showed that inhibition of histone demethylation affected the cell's ability to survive during proliferation and impaired the differentiation progression throughout the differentiation process. I also found that individual expression of target genes, such as p63 and Loricrin, showed a clear decrease in expression levels in the presence of Methylstat with a distinct dosage dependent manner. Lastly, by treating different SCC lines, I saw that cancer cells were more sensitive to lower dosages of Methylstat than normal epithelial stem cells. Overall, these results show that histone demethylation plays a large role in the regulation of proliferation and differentiation in keratinocytes. These initial findings provide a novel insight into the functionality of histone demethylation in skin and raise the possibility that histone demethylation may play a role in epithelial cancers.

Table of Contents

Background

Histones and histone modifications

A histone is a protein that allows DNA to wrap around its positively charged core to form chromatin, a vital strategy that eukaryotic cells employ to package the lengthy DNA sequence into the confined space of a nucleus (Peterson & Laniel, Current Biology, 2004). Histone proteins are highly complex due to the fact that they bind to each other to form an 8 subunit or a heteroctamer core. Histone proteins combine to make a core structure to possess two H2A and

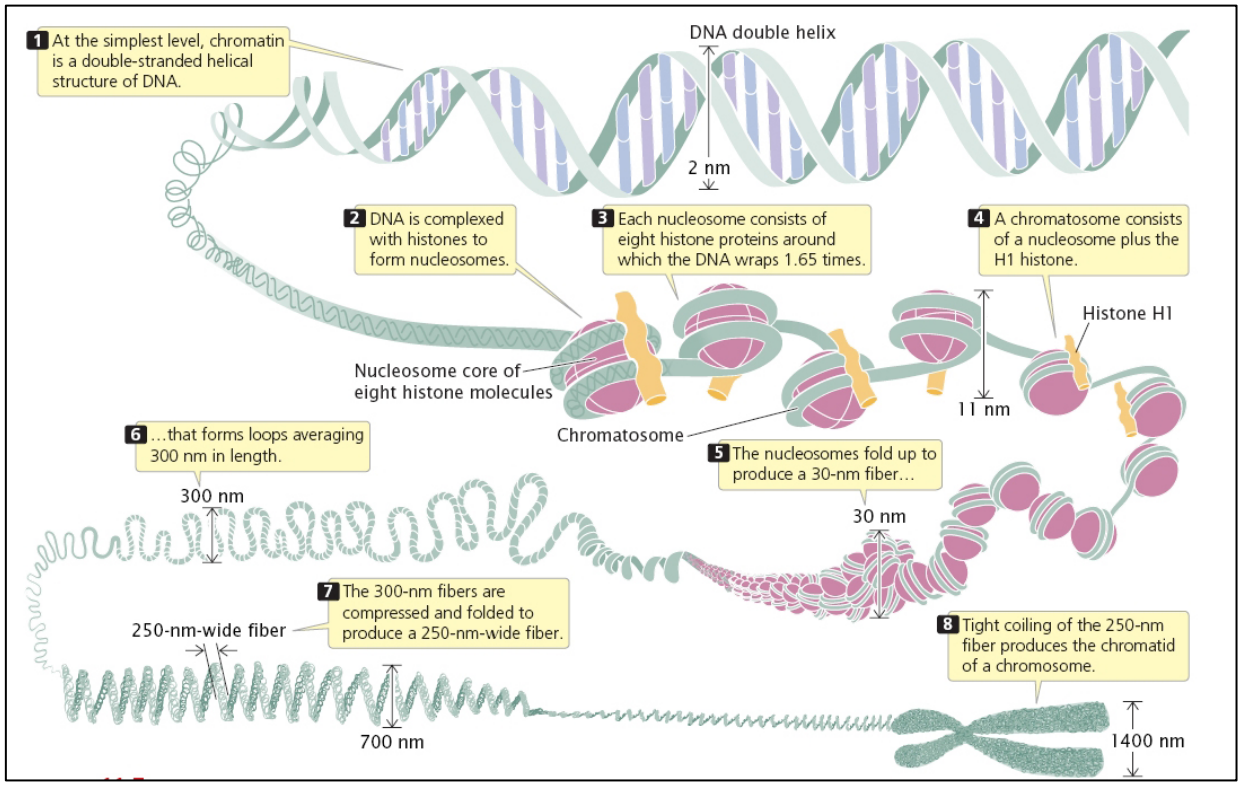

Figure 1. Compaction of DNA in the nucleus.

Diagram of how DNA packaging occurs in the nucleus and the role of histone proteins in this process (Annunziato, Nature Education, 2008).

H2B dimers and a H3/H4 tetramer of highly alkaline residues. These positively charged residues provide favorable electrostatic interactions with DNA's negative phosphate groups. Thus, DNA binds and wraps around the histone core to form a complex called nucleosome. Individual nucleosomes compact and supercoil with one other to form chromatin inside the nucleus (See Figure 1). Not only do histones play a critical role in condensing DNA, modifications to the side chains of these core proteins also provide an additional layer of control in regulating DNA-mediated processes (Peterson & Laniel, Current Biology, 2004).

Function of histone modifications

Covalent histone modifications have been well documented in science. But only recently, perhaps the past 20 years, has the functionality of these conserved modifications been truly under investigation. With a staggering amount of publications, the field of chromatin biology and related research has grown to be of significant interest, where studies show that the interaction of different types of histone modifications and small molecules can control the gene expression of certain genes that contribute to human health and disease (Sanchez & Zhou, Current Opinion Drug Discovery Development, 2009). Histone modifications, which occur post-translationally, can alter gene expression through transcriptional regulation due to the close coupling of both processes. Such modifications include acetylation, methylation, phosphorylation and ubiquitination to lysine and arginine residues that exist on the tail domains of the histone subunit proteins (Berger, Current Opinion in Genetics & Development, 2002). The modifications that occur on the histone residues can change the shape of the chromatin to either tighten or loosen the DNA wrapping around the histone core, illustrating the tight regulation of global gene expression and silencing.

Histone methylation and demethylation

Although histone acetylation has been extensively characterized, the process of histone methylation has been continually gaining scientific attention where studies show that this process may govern novel biological processes including DNA methylation, cell cycle control, transcriptional silencing and activation, and DNA repair (Guo & Guo, Proceedings of the National Academy of Sciences, 2007). Histones are methylated through an enzymatic reaction by a group of enzymes notably named methyltransferases. Methylations is known to occur on lysine residues, typically on residual sites K4, K9, K27, and K36 on the H3 subunit and K20 on the H4 subunit (Kouzarides, Current Opinion in Genetics & Development, 2002). Interestingly, methylations on different lysine residues stereotypically lead to different outcomes; for example, in mammals, H3K4[1] methylation correlates with transcriptional activation, H3K9 methylation is known to influence heterochromatin formation and gene silencing, H3K27 methylation is implicated in transcriptional repression, and H3K36 methylation is associated with actively transcribed regions (Barski et. al, Cell, 2007). This data has been highly supported through the biological academic community through the use of a highly innovative technique called Chromatin Immuno-precipitation, or ChIP, sequencing (Wang et al., RNA, 2013). This method has provided powerful information by demonstrating useful cues for gene expression changes through analysis of how proteins interact with DNA.

[1] The nomenclature for histone-modified residue is named by the histone subunit number, following with the residue (in this case, lysine) number (identified by the residue from the C-terminus), and the whether it is mono-, di-, or tri- methylation.

Before the discovery and characterization of the first histone demethylase, LSD1 (KDM1) in 2004, the scientific community deemed histone methylation deemed an irreversible process. More and more histone demethylases are continually being found and biochemically characterized. Histone demethylases (HDMs) can be broken down into two broad classes based on their enzymatic mechanisms: flavin adenine dinucleotide (FAD)-dependent HDMs and Jumonji C domain-containing HDMs (JHDMs) (Luo et. al., Journal of American Chemical Society, 2011). In general, FAD-dependent HDMs are able to demethylate mono- or di-methylated lysine residues, whereas JHDMs are less specific and so are able to demethylate mono-, di-, or tri-methylated residues.

Although the identification of these enzymes is fundamentally important, the functionality of histone demethylases provides useful information on how these enzymes contribute to biological processes. Currently, much of the functionality of these enzymes remains largely unknown. It is pertinent to understand histone demethylase function because the mechanism and sequence have been conserved from yeast to humans, prompting the importance of these enzymes in evolution; and, the recent discovery of these enzymes provides researchers a novel way of new clinical treatments that can potentially replace current practices (Tsukada et al., Nature, 2006). The fact that histone methylation is a reversible process elucidates the complexity of chromatin biology. Current opinion in the scientific community is that histone demethylation may play a role in gene expression, cell differentiation, and human diseases such as cancer (Varier & Timmers, Biochimica et Biophysica Acta, 2011). Furthermore, researchers are identifying pathways in cancer that involve histone demethylation. For example, the overexpression of a specific Jumonji-C domain-containing histone demethylase, KDM5B, is seen in bladder cancer tissue (Hayami et. al., Molecular Cancer, 2010). Additionally, since

histone methylation plays an important role in determining the activation or deactivation of particular genes without changing the genetic code, it is critical to ascertain the degree of importance of histone demethylases in the dynamic regulation of histone methylation. As such, many scientists in this field are characterizing the function of these enzymes in regards to their practicality, purpose, and their potential to become drug targets to treat human diseases.

Mammalian Skin

While histone modifications and transcriptional regulation has been shown to be relevant in many biological processes and systems, this project focuses on the effects of altering natural histone methylation processes on skin, particularly focusing on the mammalian model organism, the mouse (*Mus musculus*.)

Function and Morphology

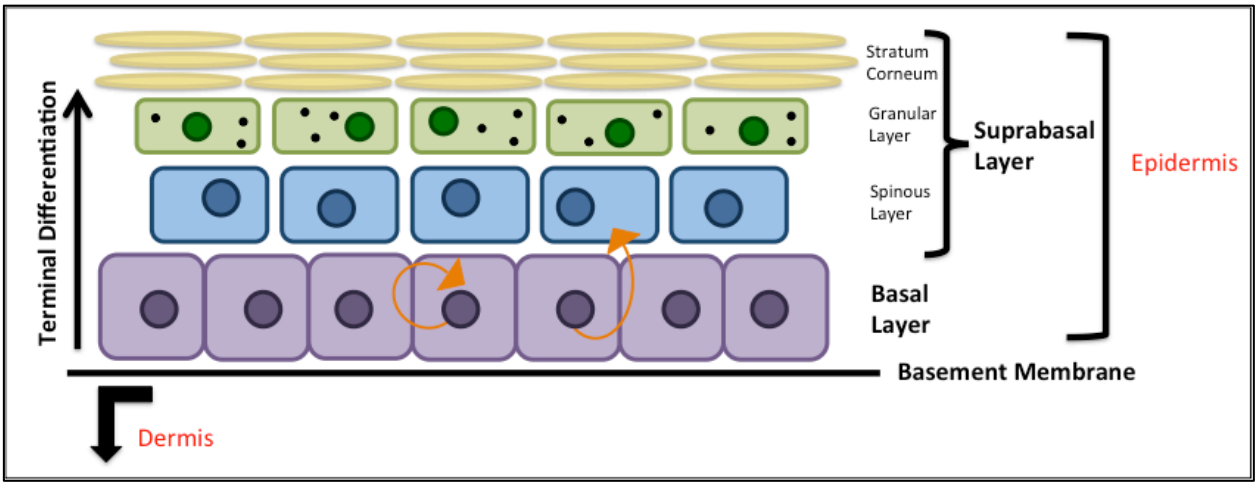

Figure 2. Morphology of an adult mammalian epidermis.

In mammals, the adult contains stratified layers of the epidermis. The basal layer, the layer closest to the basement membrane, contains stem cells that undergo symmetric or asymmetric division. Layers above the basal layer are called the suprabasal layers, where cells exit the cell cycle and undergo terminal differentiation.

The skin is the largest organ found in mammals, serving as a barrier that separates the organism from the external environment (Woodley & Freinkel, The Biology of Skin, 2001). Skin fosters a lining, either thick or thin, that allows the body to grow and protects it from potential harm. Although skin provides a beneficial protective wall for the organism, this organ also undertakes metabolic functions, stimulates sensory information, and regulates body temperature. As such, the diversity of functions that skin can perform demonstrates its versatility and resourcefulness to researchers, making it a superb model organ to study many biological processes.

In mice and many other mammals, skin is present in several intricate layers, where the outermost layer is the epidermis. This layer is useful due to its accessibility and structural organization. Each layer of the epithelium is identified by the structure of the cell body under the microscope, allowing researchers to characterize the degree to which it has differentiated (See Figure 2). The epidermis is maintained by the proliferation of a single layer of stem cells that reside in the basal layer of the epithelium. Stem cells can divide symmetrically and maintain a pool of cells that continually maintain their "stem-ness" and stay as unspecialized epidermal skin cells. Or, stem cells divide asymmetrically and give rise to differentiated cells that can migrate towards the surface and have specialized functioning, which reinforces the stratification of skin and maintains tissue homeostasis. These cells are able to leave the basal layer and enter the suprabasal layer, where they ultimately exit the cell cycle and undergo terminal differentiation (Alonso & Fuchs, Proceedings of the National Academy of Sciences, 2003).

Epidermal Proliferation and Differentiation - Morphogenesis

The epidermis is maintained through a balance of stem cell proliferation and terminal differentiation of cells with specific roles. During embryonic development, a single layer of basal

cells give rise to the epidermis, hair follicle and sebaceous gland through a wide array of regulated pathways (Yi and Fuchs, Cell Death & Differentiation, 2010). By adulthood, these three populations of skin cell lineages are constantly renewed through proper homeostasis, which continues the pools of proliferative cells and regenerates differentiated and distinct cell-types (See Figure 3).

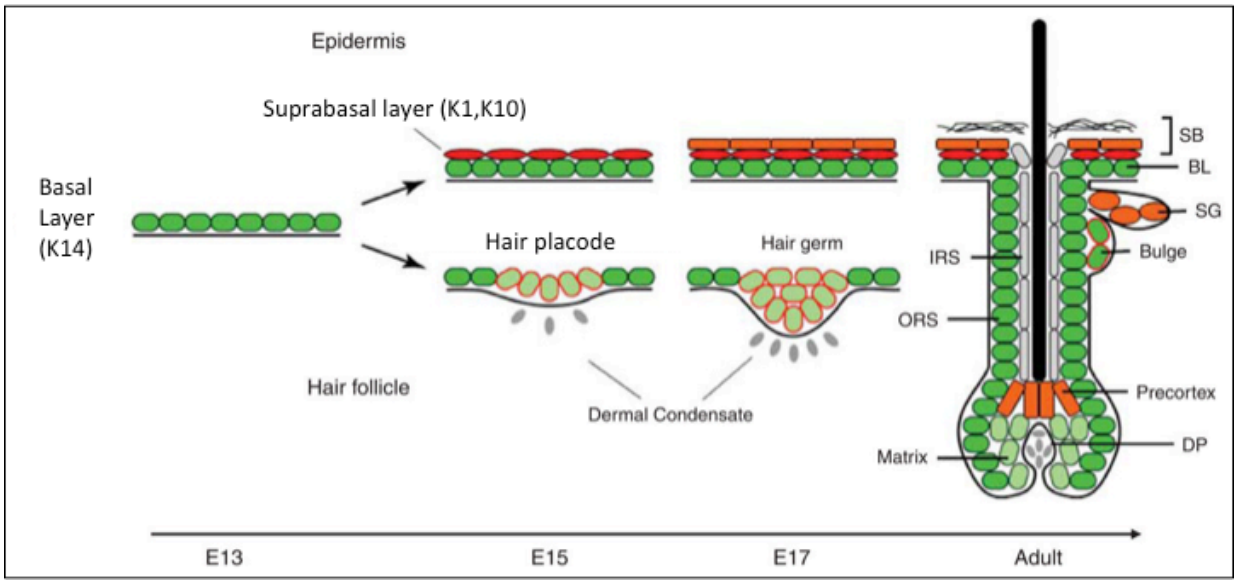

Figure 3. Illustration of embryonic epidermal development and hair follicle formation.

In mammals, the epidermis consists of a single layer of cells at embryonic day 13. By embryonic day 15, the single layer of cells gives rise to the suprabasal layer and subsequent layers arise later in development (Yi and Fuchs, Cell Death and Differentiation, 2010).

Through the development of the skin, different cells are "assigned" different roles. Each role carries out a different function to help develop the skin and hair follicle. Cells can either undergo terminal differentiation, where they carry out their job and have no self-renewal capacity, or remain non-specific and can replicate. (See Figure 4 for cellular lineages and specified differentiated populations).

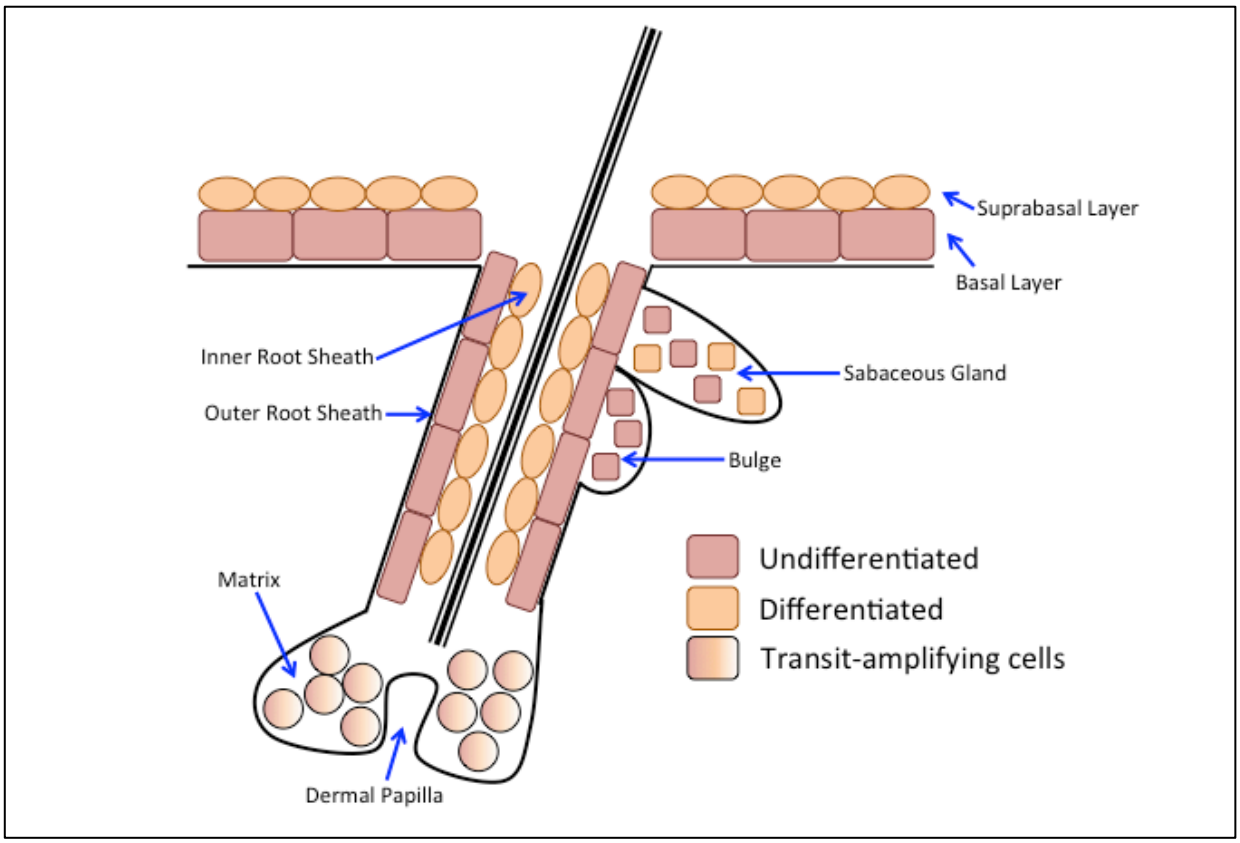

Figure 4. Epithelial cell lineages.

This diagram shows the different cell lineages in the mammalian skin and their state of differentiation. The red cells represent cells that are undifferentiated and undergoing the cell cycle. The bulge region and the basal layer constitute cells that are replenishing the hair follicle and interfollicular epidermis. The orange cells represent cells that are terminally differentiated. These cells cannot renew themselves and have a specific role in the skin. Cells in the sebaceous gland are either differentiated or proliferative. Lastly, the matrix cells contain unique cells that are transit-amplifying cells, meaning that they are constantly dividing and differentiating simultaneously.

The major structural proteins of the epidermis are keratins, intermediate filaments that help anchor the epidermis to its base and maintain tight contact between epithelial cells. Typically, keratins that are expressed in the basal layer are K5 and K14, and keratins that are expressed in the intermediate suprabasal layer (spinous layer) contain keratins K1 and K10. Although the molecular mechanisms involving the differentiation pathway of keratinocytes

remain mostly unknown and controversial, there is some evidence that p63, a transcription factor, is involved in the process of epidermal stratification (Blanpain and Fuchs, Annual Review Cell Developmental Biology, 2006).

Squamous cell carcinoma

Squamous cell carcinoma (SCC) is a cancer that originates from epithelial keratinocytes, the most abundant epithelial cell type in the body. It is one of the most common cancers and has the ability to grow on any anatomical location on the body. Moreover, organs other than skin mostly contribute to the commonality of squamous cell carcinoma- for example, nearly all lung cancers are squamous cell carcinoma, with some exceptions (Goldman, Seminars in Cutaneous Medicine and Surgery, 1998). As such, this type of cancer is of high interest to researchers due to the vulnerability humans have to the disease. Malignant tumors that arise from squamous cell carcinoma are quite biologically aggressive and can recur with an even more rigorous metastatic behavior than the cellular carcinogenesis previously (Goldman, Seminars in Cutaneous Medicine and Surgery, 1998). Unlike almost all basal-cell carcinomas, another non-melanoma skin cancer, cutaneous squamous cell carcinoma is associated with considerable risk of metastasis (Alam & Ratner, The New England Journal of Medicine, 2001).

The risk of obtaining squamous cell carcinoma comes down to two factors: amount of sun exposure and degree of pigmentation. Usually, fair-skinned individuals are more prone to acquiring this disease than dark-skinned individuals, but it is not uncommon for someone with dark skin to get squamous cell carcinoma. Although squamous cell carcinoma can appear in a variety of morphologies, it is characteristically seen as raised, firm, pink to flesh-colored keratotic papule. Due to the fact that it can recur, has metastatic properties, and carries a poor

prognosis, quick excision and early clinical treatment are best to prevent the spread of the cancer (Goldman, Seminars in Cutaneous Medicine and Surgery, 1998).

For this thesis study, squamous cell carcinoma cell lines are used to test the effectiveness of a small molecule in order to inhibit histone demethylase function, Methylstat, to see the degree of sensitivity these cells have to the drug. Additionally, the squamous cell carcinoma cell lines allow us to gain vital information regarding the dosage compensation of the drug *in vitro*. Although all of the cancer cells lines used in this study come from the same histology type, meaning that they stem from the same type of cancerous disease, each cancer cell line have differences in morphology, chromosomal make-up, resistance to drug therapies, and degree of differentiation. As such, we selected three different SCC cell lines to be treated with Methylstat: Cal-27, SCC-4, and SCC-13, to represent the diverse course of cancer cells within one type of histology.

Cal-27

Cal-27 cells are human squamous cell carcinoma cells, originating from the tongue. They were taken from the middle third of the tongue of a 56-year old Caucasian male. These cells are peculiar in that they have rapid proliferation but their morphology is similar to that of differentiated epithelial (polygonal) cells. The significance of their morphology being similar to differentiated cells, yet having high proliferation is due to the fact that normal differentiated cells do not have the capacity to replicate and divide at the same fast pace. Cal-27 cells are considered tumorgenic in athymic nude mice, so they are able to form tumors in mice with a compromised immune system. Cal-27 was specifically chosen to undergo Methylstat treatment due to its differentiated morphology, which provides insight on squamous cell carcinoma cancers that

bears resemblance to differentiated epithelial cells (Gioanni et al., European Journal of Cancer and Clinical Oncology, 1988).

SCC-4

SCC-4 cells are also a human squamous cell carcinoma line that originated from the tongue. They were extracted from a 55- year old male. These cells have an undifferentiated morphology with characteristics that are similar to keratinocytes, but contain the highest heterogeneity in shape of all the cell lines used in this experiment, as well as the greatest average colony size. Like Cal-27 cells, SCC-4 cells are also considered tumorgenic. SCC-4 cells grow substantially better with 3T3 (fibroblast) feeder cells, which were not used in this experiment. SCC-4 cells were an evident choice for this experiment, because its undifferentiated morphology provides more information on squamous cell carcinoma resembling proliferative epithelial cells (Rheinwald and Beckett, Cancer Research, 1981).

SCC-13

SCC-13 cells are human squamous cell carcinoma cells that originated from the facial epidermis (also known as head and neck squamous cell carcinoma). These cells were from a 56-year old female who had received a series of radiation treatments for the tumor several years before its surgical removal. These cells have a differentiated type of morphology that also pertain to epithelial-like cells. Similar to SCC-4 cells, SCC-13 cells grow markedly better with feeder cells present (with almost complete dependence), however feeder cells were not used in this experiment to prevent acquisition of clones of differentiated cells. Since SCC-13 has medial characteristics similar to both Cal-27 and SCC-4, these cells were a viable choice for this

experiment to show the effects of Methylstat on a squamous cell carcinoma line that contains features of the other two lines (Rheinwald and Beckett, Cancer Research, 1981).

The histone demethylase project

Jumonji C domain-containing histone demethylases (JHDMs) are the largest class of histone demethylase enzymes that catalyze lysine demethylation on histones, utilizing a metal ion co-factor, Iron (II), to transform their substrate to product (Tsukada et al, Nature, 2006). In addition to the metal cation, JHDMs also use α-ketoglutarate as a co-factor, constraining their mechanism to be somewhat complex. Enzymes that contain the Jumonji-C domain (JmjC) fold into eight β-sheets, which form the enzymatic pocket and serve as the active center for demethylating the basic residue (Klose, Nature Reviews Genetics, 2006). JHDMs prove to have a broader range of specificity, because they can demethylate tri-methylated residues. So far, their substrates have been reported to be residues on histone 3: H3K4, H3K9, H3K27, and H3K36 (Klose, Nature Reviews Genetics, 2006).

There are many classes of JHDM enzymes that are found throughout the phylogenic kingdom, from budding yeast to humans (Shi & Whetstine, Molecular Cell Review, 2007). Based on the structural relationships of the JHDM classes and other domains identified on these demethylase proteins in chromatin biology, it is possible that they involve a variety of functions that when mutated, can serve as potential links to mental retardation, Y-chromosome defects, and congenital alopecia or baldness (Klose, Nature Review Genetics, 2006). Therefore, although histone demethylases are widely known to counteract histone methylations, the potential that they have for multi-functionality is large and worth studying to find treatments for human diseases.

Methylstat, the drug

The study of histone modifications in the mouse genome can be complicated due to the fact that mice have enzymes that can be grouped into categories and have similar functionality. As such, the redundancy of enzymes makes loss-of-function experiments uninformative, because knocking out one gene may not give expected results, as another enzyme can compensate for the knocked-out gene. Therefore, small molecules have been extensively used throughout the scientific community in model organisms to identify the structure and function of certain enzymes due to the limitations of other techniques to not only characterize the enzymes, but also to possibly discover new treatments for diseases such as cancer. In 2011, the Wang Lab (Luo et al.) in the department of Chemistry and Biochemistry at the University of Colorado at Boulder published a journal article about the synthesis of a promising small molecule that targets a Jumonji C domain-containing HDMs (Luo et al., Journal of the American Chemical Society, 2011). The small hydrophobic molecule is called the Methylstat (see Figure 5 for structure of

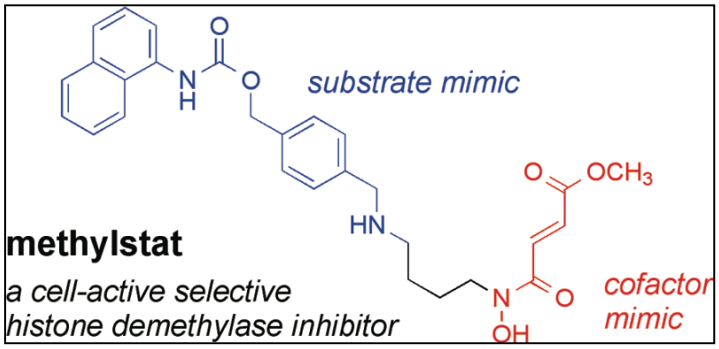

Figure 5. Molecular structure of Methylstat.

Methylstat is a transition state analog that has broad specificity for histone demethylase enzymes with the Jmj-C domain (Luo, Journal of American Chemical Society, 2011).

molecule), where it is designed to contain regions that mimic the lysine substrate and the α-ketoglutarate co-factor, thus the molecule imitates the transition state of the substrate-enzyme complex. There is data that validates the novelty of the drug, Methylstat, from the cell culture work described in the article, suggesting that it can potentially become a unique pharmaceutical

ENZYME	SUBSTRATE	IC_{50} (µM)
JHDM1A	H3K36me2	0.40
JMJD2A	H3K9me3	4.3
JMJD2C	H3K9me3	3.4
JMJD2E	H3K9me3	5.9
JMJD3	H3K27me3	10
PHF8	H3K9me2	43
LSD1	H3K4me2	620
HDACs	$K_{acetylated}$	>800
PHD1	$P_{hydroxylated}$	54
PHD2	$P_{hydroxylated}$	83
PHD3	$P_{hydroxylated}$	31
FIH	$N_{hydroxylated}$	22

Figure 6. IC_{50} data on Methylstat.

The IC_{50} data gives insight on the specificity of the Methylstat drug to JHDMs. The Wang lab at the University of Colorado at Boulder tested the specificity of Methylstat to different kinds of endogenous enzymes. The table shows that Methylstat is highly specific to enzymes that contain the JmjC domain in the active site, and JMJDs, which are specifically JmjC enzymes that are histone tri-demethylases. To compare Methylstat treatment with other enzymes, they included enzymes that are JmjC-domain containing histone demethylases but for di-or monomethylated lysine residues, flavin-dependent histone demethylase, histone deaceytlases, and Fe(II)-dependent hydroxylases (Wang Lab, University of Colorado at Boulder, unpublished data, 2011).

agent for diseases that involve histone demethylases. The most recent data acquired on this small molecule suggests that it has high selectivity for JHDMS. The Wang Lab examined the specificity of this drug by researching the IC_{50} values of the drug for JHDMs in comparison to other enzymes with similar functionality or mechanisms in a strain of human esophageal squamous cell carcinoma cell line, KYSE 150 (See Figure 6). IC_{50} values are the half maximal inhibitory concentration, which shows the amount of drug needed to inhibit the function of half of the concentration of the enzyme present. From Figure 6, Methylstat proves to have high specificity to JHDMs, where the amount of drug required to inhibit these demethylases are substantially less than the other enzymes on the list. Due to its high specificity to Jumonji-C-

domain-containing histone demethylases, Methylstat is a promising choice to have a better understanding of histone methylation and demethylation in mammalian skin and the impact of such processes on the proliferation and differentiation of the epidermis.

Approach to studying histone demethylation and target genes

This project aimed to explore the functional role of histone demethylation in regulation of proliferation and differentiation pathways in the skin. This project accomplished this aim by studying histone methylation accumulation *in vitro* by treating murine epidermal keratinocytes with Methylstat to study the effects of histone demethylation inhibition on lineage differentiation. This project helped further elucidate the morphological changes in keratinocytes by examining proliferation and differentiation processes, depicting how the removal of a broad range of demethylases can affect the overall fate of a cell. Ultimately, this project provided a fundamental understanding of the effectiveness of Methylstat in keratinocytes and directly analyzed the functional study of histone demethylation on skin stem cell differentiation and proliferation. It is hypothesized that altering the modulation of histone methylation will change the fate of the cell. To accomplish this, wild-type keratinocytes were obtained from newborn mice to culture *in vitro* under proliferative and differentiated conditions with varying concentrations of Methylstat. We examined the proliferation and differentiation of these keratinocytes by depicting the changes in the cell cycle progression of the cells via flow cytometry to generate cell cycle profiles and by seeing how the gene expression level of certain markers of proliferation and differentiation changes with added drug via qPCR (quantitative polymerase chain reaction). Additionally, Methylstat was added to human squamous cell carcinoma cell lines to see the degree of effectiveness of the drug at repressing cancer cell growth *in vitro*.

Cell culture system of keratinocytes

Numerous landmarks have been achieved due to the development of cell culture. It is a technique that allows a researcher to grow cells isolated from an organism under controlled conditions that help maintain the same biological processes found within their natural environment. It is typical to consider cell culture conditions to be *in vitro* work, because the cells are being kept alive in a petri dish and not by the host organism. As such, cell culture has given scientists the ability to gather information about certain biological activities and mechanisms through a relatively cheap and simple methodology. This project primarily focuses on the isolation of keratinocytes from newborn, wild type mice, and culturing these cells with varying conditions to observe morphological or phenotypic changes. This project cultures the acquired keratinocytes in media with low or high calcium conditions to observe and analyze changes in cell fate with the induction of Methylstat (Hennings et. al, Cell, 1980). High calcium conditions in media can induce differentiation in epithelial stem cells, in vitro, because calcium is required for the reorganization of the cytoskeleton to form intracellular junctions and desmosomes that leads to stratification of epithelial cells (Lewis et al., The Journal of Investigative Dermatology, 1994). Furthermore, different squamous cell carcinoma cell lines are also utilized to see morphological changes with the induction of the drug so that more information can be gathered about the degree of sensitivity different kinds of cells has to the drug.

Western Blot Analysis

The western blot assay is an analytical technique used to identify key proteins in a given sample of cells. Western blots transfer proteins onto a membrane that holds the proteins and utilizes antibodies that stain for the desired protein. These assays are a critical component to this experiment, because they verifies that Methylstat is effective not only in the cell line used in the

literature, but also in keratinocytes. Plus, these assays provide quantitative information on histone methylation accumulation with different concentrations of Methylstat added. We utilized Western blots to show that accumulation of histone methylation actually occurs in not just cancer cells described in literature (Luo et al., Journal of the American Cancer Society, 2011) but also occurs in keratinocytes; and to show that higher dosages of Methylstat increases accumulations of histone methylation in a dosage response manner in keratinocytes. In this experiment, β-Tubulin antibody is used as a loading control, where H3K9me3 and H3K36me2 antibodies are used to quantify histone methylation accumulation due to the high sensitivity the histone demethylases are for these markers (Luo et al., Journal of American Chemical Society, 2011).

β-Tubulin Antibody

β-Tubulin is a protein that helps make up microtubules in the cell. This protein provides a useful positive control because it is present at relatively equal levels in every cell, allowing us to see that the variations in histone accumulation is in fact due to the drug and not because of product availability.

H3K9me3 Antibody

H3K9me3 is a tri-methylated lysine residue on histone 3. This marker mediates gene silencing and is known to be regulated by Jumonji-C containing domain histone demethylases (Lu et al., Cell Cycle, 2009). Additionally, Methylstat has been shown to have high specificity histone demethylases that modulate this marker: JMJD2A, JMJD2C, and JMJD2E (Luo et. al., Journal of American Chemical Society, 2011). Lastly, current research shows that overexpression of JMJD2C is seen in esophageal squamous cell carcinoma (He et al., Acta

Biochimica et Biophysica Sinca, 2012), so the fact that Methylstat has great potential in blocking these histone demethylases supports the choice of this antibody in this project.

H3K36me2 Antibody

H3K36me2 is a di-methylated lysine residue on histone 3. This methylation marker is known to facilitate actively transcribing genes and also regulated by JHDMs. Specifically, H3K36me2 methylation mark is regulated by the histone demethylases JHDM1A and JMJD2, yet little is known about these HDMs (Klose & Zhang, Nature Reviews, 2007). Overall, H3K36me2 was chosen as a marker for this project due to the fact that it contains the highest sensitivity to Methylstat with an IC_{50} value of 0.40 μM (Wang Lab, University of Colorado at Boulder, unpublished data, 2011).

Cell cycle analysis

One of the most vital methods used in these experiments was evaluating the cell cycle profiles of different cell populations through flow cytometry. Analyzing the cell cycle state of a population of cultured cells gave us an idea of the state of proliferation. Movement through the cell cycle is a highly regulated process, and its complexity is divided into several phases (See Figure 7). The rate of progression through the cell cycle is an important factor in determining the proliferative ability of a population of cells. One of the most important factors of the cell cycle is DNA replication, and because of this, changes in the amount of DNA allow us to quantify the progression of the cells through the cell cycle in an easy and quick manner. In this project, DNA staining dyes and incorporation of Bromodeoxyuridine (BrdU) are utilized to explore cell cycle progression and analyze proliferation of these cells when exposed to different concentrations of Methylstat.

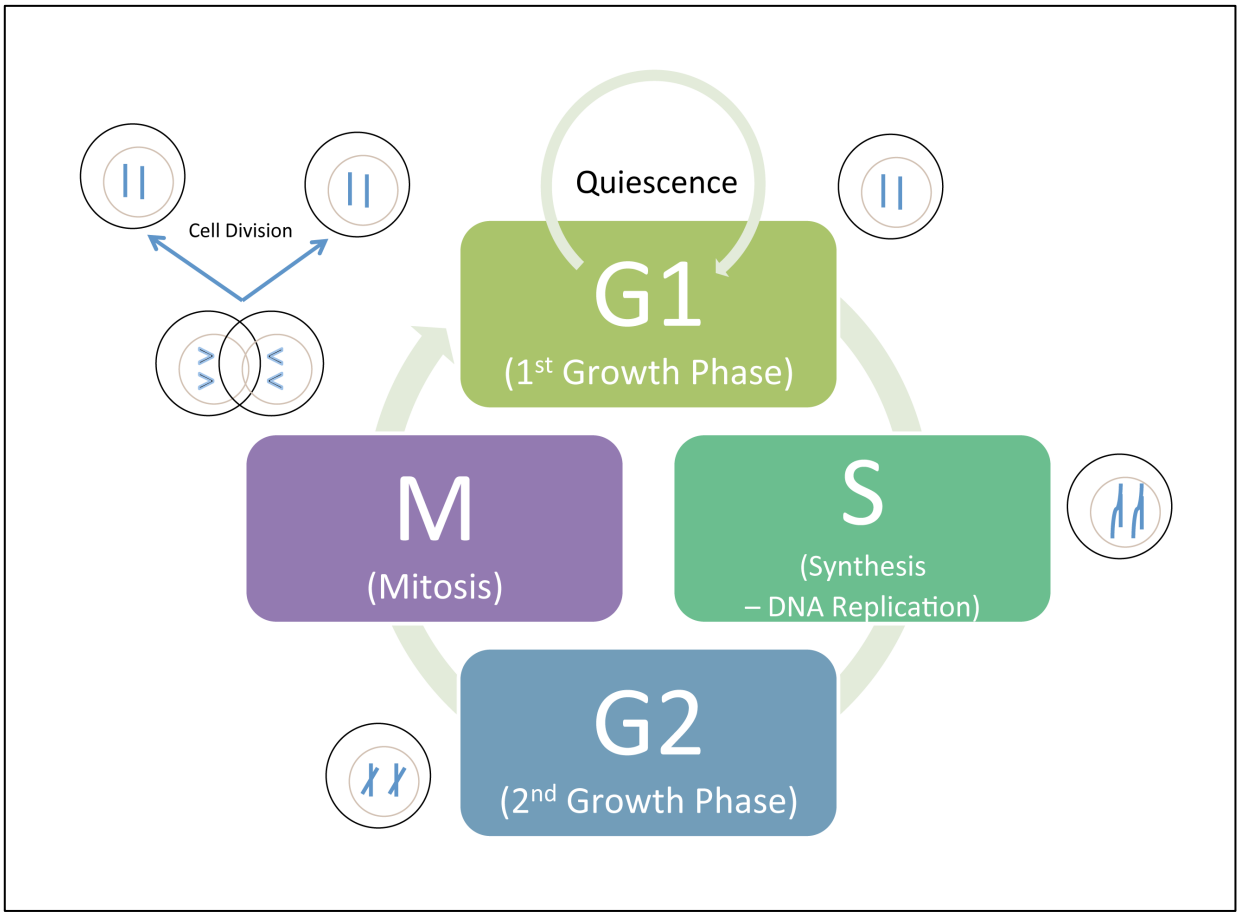

Figure 7. Schematic diagram of cell cycle.

The cell cycle is divided into five phases: G0, G1, S, G2, and M. G0 is known to be for quiescent cells. G1 is the first growth phase. During the G0 and G1 phase, cells are diploids, so they only contain 1 copy of the chromosome. S is the DNA synthesis phase, where the DNA is replicated. G2 is the second growth phase. M is mitosis. During the G2 and M phase, the cell contains two copies of their chromosome. After the M phase, the cell recycles back to the G1/G0 phase.

Propidium iodide (PI) and Hoechst dye DNA-staining

A simple version of cell cycle analysis is done by staining the DNA to measure the amount of DNA in the cell, where the amount of fluorescence correlates to the amount of DNA. We used propidium iodide (PI), which is an intercalator of DNA and RNA that enhances fluorescence upon binding. We added the Propidium Iodide after fixation of the cells with 100% ethanol. We used flow cytometry to measure the fluorescence. In this way the cell cycle profile

can be generated, where the profile indicates the cell-cycle state of each cell as well as the population as a whole.

Another DNA-staining dye used in this experiment is Hoechst dye. Similar to PI, Hoechst dye quantitatively binds to DNA, and upon binding, fluorescence increases and can be measured through flow cytometry. However, Hoechst dye binds through a mixture of intercalation and minor-groove binding modes. Due to its binding properties, Hoechst dye provides more clear and neat cell cycle profiles when BrdU incorporation is utilized in comparison to propidium iodide. As shown in Figure 8A, a cell cycle profile generally shows two peaks, where the fluorescence of the second peak is normally twice as intense as the first peak. The first peak is indicative of the G0-G1 phases, where there is only one copy of chromosomal DNA and the second peak is indicative of the G2-M phases, where there are two copies of chromosomal DNA. The region in between the peaks corresponds to cells in the S phase, where cells are in the process of replicating their DNA.

BrdU (Bromodeoxyuridine) Labeling

Bromodeoxyuridine (BrdU) is a thymidine analog, synthesized by the replacement of a bromine atom for thymidine's methyl group. BrdU is commonly used in cell cycle analysis assays, because during replication, the cell's machinery can mistake BrdU for thymidine and incorporate the analog into DNA. So, fluorescent antibodies can be used to recognize the present of BrdU in genomic DNA. The utilization of BrdU supplements cell cycle analyses conducted with DNA-staining protocols, because it allows us to further separate S phase cells from the other two populations, since BrdU can only be detected when cells are replicating their DNA. In a BrdU profile (shown in Figure 8B), the histogram usually shows two peaks that are distinctive of BrdU positive (S phase cells) and BrdU negative (cells in the other four phases) cells from the

intensity of the fluorescence on the BrdU antibody. Figure 8C shows that BrdU cells can be also stained with a DNA-staining dye to create a cell cycle profile to distinctively separate G0-G1, S, and G2-M cell populations.

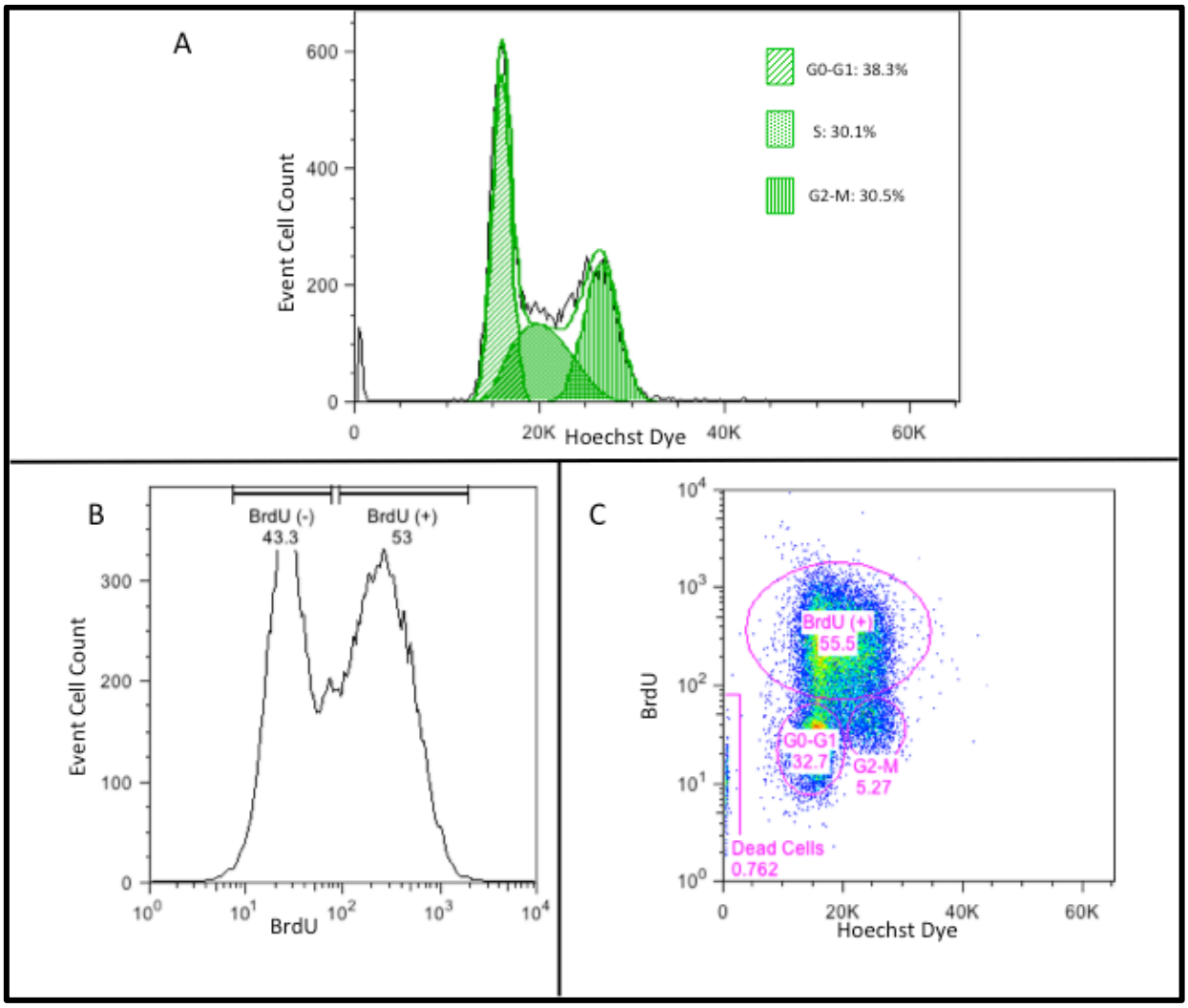

Figure 8. Cell Cycle Profile.

A. This plot shows a cell cycle profile with Hoechst dye and representative of a cell cycle profile with PI staining, showing G0/G1, S, and G2/M distributions. **B.** BrdU histogram demonstrating the distribution of positive (BrdU (+)) and negative (BrdU (-)) cells. **C.** A cell cycle profile plotted BrdU against Hoechst Dye, with gating for G0/Gl, G2/M, BrdU positive cells, and dead cells.

The purpose of BrdU is to label cells that are undergoing DNA replication. However, in the use of BrdU, we pulse the cells in cultured media with BrdU for only a limited amount of time. As such, the cells that are undergoing DNA replication in the S phase but are absent from BrdU labeling will not be included in the profile. While BrdU labeling for cell cycle analysis is a valuable tool, it only provides a general idea of the proliferative cells in the population.

Histone Demethylation Targets (qPCR)

One of the main goals of this experiment was to see how different genes change expression levels from the reduction of histone demethylation in cells. Quantitative polymerase chain reaction (qPCR) was used to carry out this analysis. This technique, also known as real-time PCR, is a method that is an essential way to identify specific gene targets that are affected by the absence of histone demethylation. Quantitative-PCR is a technique that is based on the original polymerase chain reaction technology, which functions to amplify specific gene products in a population of cells. Oftentimes, qPCR is combined with the enzyme, reverse transcriptase, to amplify messenger-RNA (mRNA) products into complementary-DNA (cDNA) due to the higher stability of DNA in comparison to RNA to conduct the analysis. As a result, the amplified products can be quantified and different populations of cells can be compared with one another, based on the amount of the specific gene targets. In this project, qPCR was utilized in conjunction with reverse transcriptase to quantify the mRNA gene products of four specific genes. We chose four gene targets to study: two proliferation-specific (basal cells) marker, two differentiation-specific (suprabasal cells) markers. These were chosen because not only are they important for proliferation and differentiation pathways in epithelia, but they are also involved in cellular carcinogenesis. These targets include K14, p63, K1, and Loricrin.

K14

Keratin-14 (K14) has been well documented in the literature as a biochemical marker of stratified squamous epithelia. Specifically, K14 is used to mark proliferative cells in the basal layer. In general, the expression patterns of K14 exist in mitotically active cells, which coincides with pluri-potency and undifferentiation (Coulomb et al., The Journal of Cell Biology, 1989). As such, K14 was chosen as a target in this experiment to quantitatively see the proliferative ability of the cells with different concentrations of Methylstat treatment.

p63

The protein p63 is a transcription factor and also a homologue of the tumor suppressor gene p53 (Yang et. al., Nature, 1999). This gene is not only important for limb and skin epidermal development (Truong et al., Genes & Development, 2006), but its expression is also associated with processes such as apoptosis, cellular proliferation, epithelial terminal differentiation, and cellular adhesion (Lau et. al., International Journal of Oncology, 2012). In the interfollicular epidermis, p63 is expressed primarily in the basal layer. Due to its involvement in cellular proliferation and epithelial terminal differentiation, p63 was a clear choice for a target gene for this study.

K1

Keratin-1 (K1), along with Keratin-10, is a predominant intermediate filament cytoskeletal protein that is present in differentiated epithelium, specifically expressed in the spinous and granular layers (Huber et. al., Journal of Investigative Dermatology, 1994). Changes in epithelial cellular morphology from proliferation to differentiation states are known to be associated with such keratin proteins. Changes in the level of K1 are indicative of functional

changes to genes that allow differentiation to occur in mature epithelial cells. As such, K1 was chosen as a gene target in this project to determine the changes in levels of these proteins with various concentrations of Methylstat treatment.

Loricrin

As mentioned earlier, the stratification of skin allows for the suprabasal layer to have minor layers with different degrees of differentiation. Depending on how differentiated a cell is in the skin, different proteins will be present, so the use of one biochemical marker of differentiation does not give enough insight on the degree of differentiation. Loricrin is a protein that is produced from the LOR gene and is a major component of the cornified epithelium or stratum corneum (Nishifuji and Yoon, Vet Dermatology, 2013). . Generally, both K1 and Loricrin have been proven and accepted by the scientific community as viable markers of keratinocyte differentiation (Li et al., RNA, 2013). Since Loricrin also marks terminal differentiated epithelial cells, it was chosen as a marker for late-stage differentiation

FoxN1^{ex9Cre}/R26R^{LacZ} transgenic mice

Although the use of an *in vitro* system provides valuable information about the impact of histone demethylation on epidermal proliferation and differentiation, not all questions can be answered via this methodology. We look forward to employing the use of transgenic mice, an *in vivo* system, to further understand cellular differentiation in the interfollicular epidermis and how inhibition of histone demethylases can potentially influence this process.

The gene FoxN1 encodes for a transcription factor that is active in the thymus and cutaneous tissues. Mutations of FoxN1 produce a nude phenotype in mice and humans (Janes et al., Journal of Cell Science, 2004). This transcription factor is known to activate genes that are

required for follicular differentiation of epithelial cells, so using this gene to mark epithelial terminal differentiation can provide significant insight into the lineage of differentiation in mouse skin. We obtained a transgenic mouse line that has a knocked-in cassette for Cre recombinase on the 3'-UTR of the FoxN1 gene. This transgenic mouse was created by the electroporation of a vector that contained the FoxN1-gene sequence with an IRES-Cre insertion in the 3'-UTR section of the gene. IRES stand for internal ribosomal entry site, which is a nucleotide sequence that allows for cap-independent translation of a "middle" section of the mRNA sequence– so, in this case, translation of Cre can occur without it having its own transcript (Mizuguchi et al., Molecular Therapy, 2000). The Cre recombinase expression allows for visual detection of differentiated cells by mating this transgenic mouse to another transgenic mouse that has a knockout allele that is driven by the Rosa-26 promoter. This null allele on the second transgenic mouse contains the reporter gene, LacZ that is flanked by loxp sites. When both of these transgenic mice are mated, the loxp sites are recombined by Cre recombinase in the progeny, allowing for the expression of β-galactosidase from the LacZ gene (see Figure 9). Thus, the progeny's skin epithelium can be stained to show the suprabasal layers in the interfollicular epithelium using X-gal and hematoxylin.

X-gal

X-gal is an abbreviation for 5-bromo-4-chloro-indolyl-β-D-galactopyranoside, a synthetic compound that consists of galactose attached to an indole ring. X-gal is commonly used to detect the active enzyme β-galactosidase in cells. X-gal itself is a colorless compound, but when bound to the enzyme, an intense blue color appears (Horwitz et al., Journal of Medicinal Chemistry, 1964). Therefore, the use of X-gal will show where β-galactosidase is present in the tissue, allowing us to know where FoxN1 is primarily transcribed in skin.

Hematoxylin

Hematoxylin is a natural dye compound that is obtained from logwood and is frequently used to stain tissues based on their histology (Avwioro, Journal of Physics and Chemistry of Solid, 2011). In this experiment, hematoxylin is used as a nuclear counter stain to provide a better view of the skin's stratified structures.

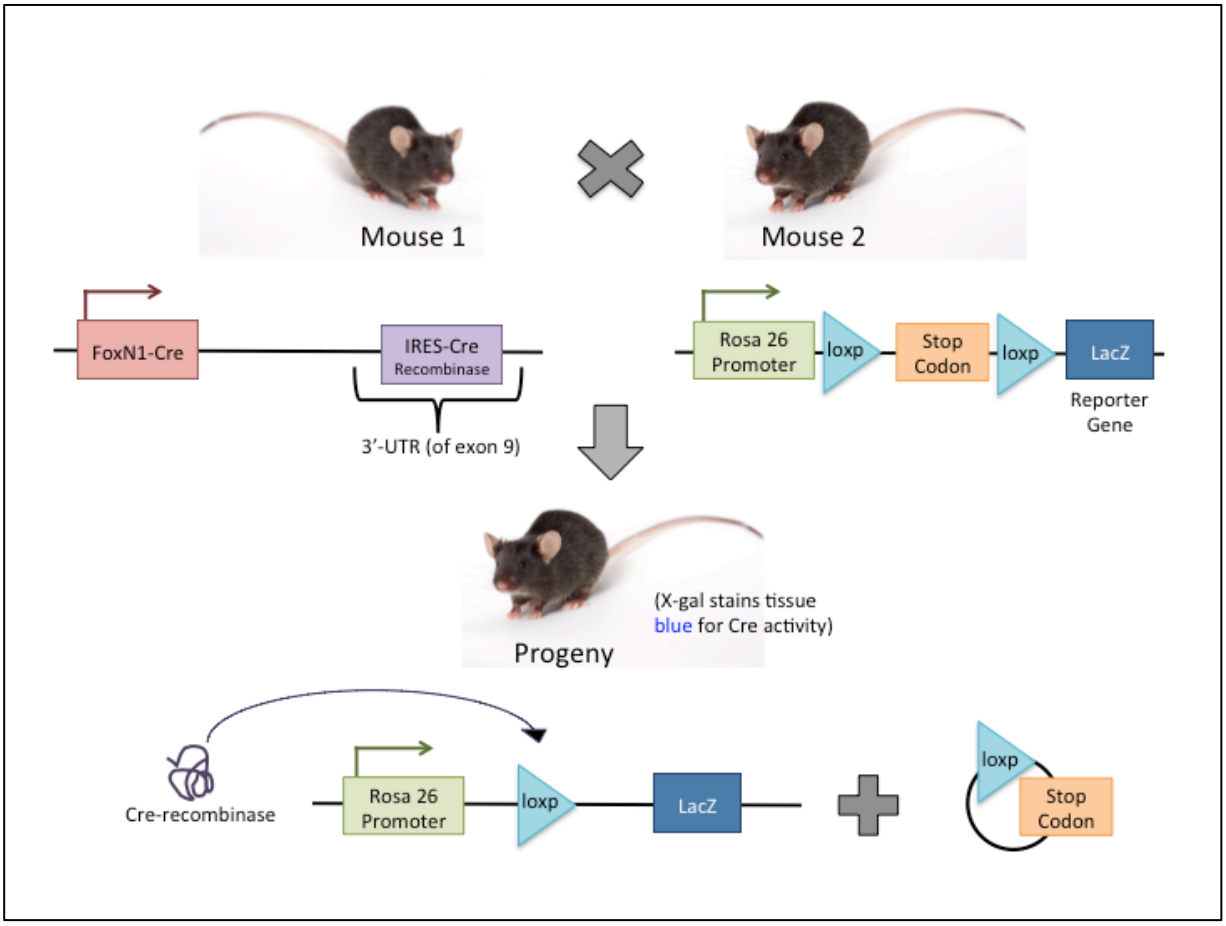

Figure 9. Diagram representation of knock-in mouse crossing of FoxN1-Cre and Rosa 26 reporter.

Mouse 1 has a genotype containing the FoxN1-Cre allele, where expression of FoxN1 will cause a Cre recombinase expression through the insert of an IRES-Cre in the 3'-UTR. Mouse 2 has a genotype containing the reporter gene, LacZ, driven by a Rosa 26 promoter and flanked by loxP sites. Therefore, once Mouse 1 and 2 are mated, the progeny will have expression of LacZ to yield the active enzyme, β-galactosidase, if the FoxN1-Cre allele is expressed in the terminally differentiated layers of the mammalian epithelium.

Results

Morphological changes in cells with Methylstat treatment

Methylstat caused decrease in cellular growth and enhanced apoptosis in proliferative keratinocytes, differentiated epithelial cells, and human squamous cell carcinoma cells.

To determine the morphological changes that occur when cells were treated with Methylstat, we took pictures under a bright-field microscope of cells that were treated with different Methylstat concentrations. At first, we needed to establish a dosage range that did not kill off the cells but still provided a noticeable phenotype. We found that with keratinocytes, severe phenotypic changes occurred in a small dose range: 2 μM to 4 μM. We saw significant cell death and decreased cellular growth by 4.5 μM Methylstat treatment.

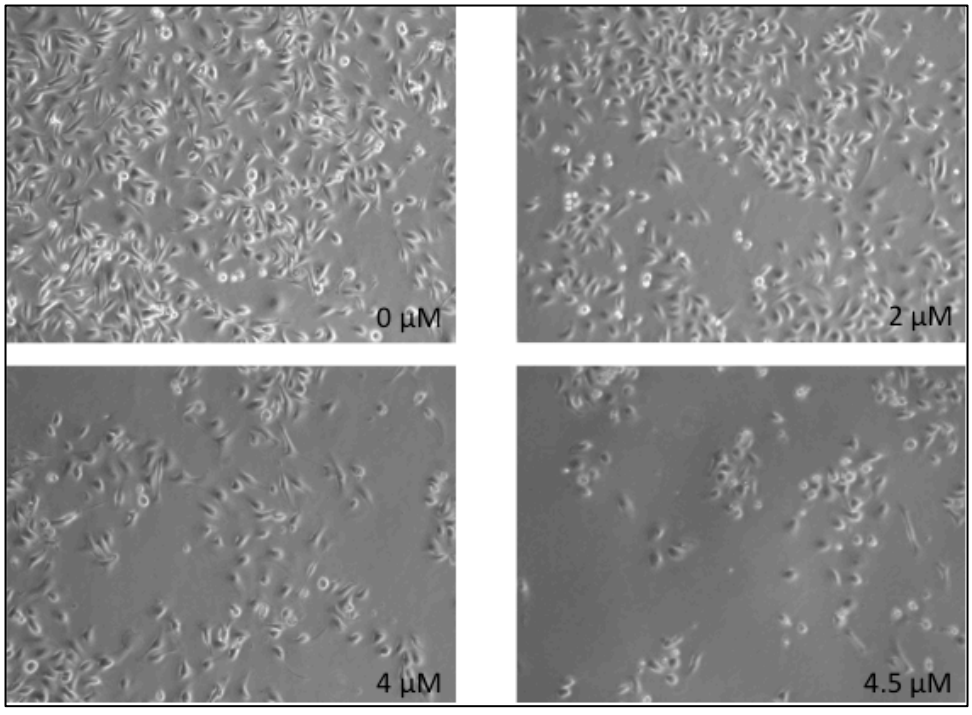

Figure 10. Phenotypic changes in keratinocytes with Methylstat drug treatment.

With higher dosages of Methylstat drug treatment on keratinocytes, apoptosis and decrease in cellular growth was observed under the light microscope.

The fact that there were significant phenotype changes within the small dosage range of Methylstat use, we preformed another experiment by differentiating the proliferative cells 24 hours after Methylstat treatment to see if there were similar morphological changes in the cells. Again, we looked into the morphological changes of these differentiated epithelial cells to observe that these cells had the same phenotype as the proliferative cells with a similar dosage dependent response. We determined that adding Methylstat prior to differentiation also causes a decrease in cellular growth and enhanced apoptosis.

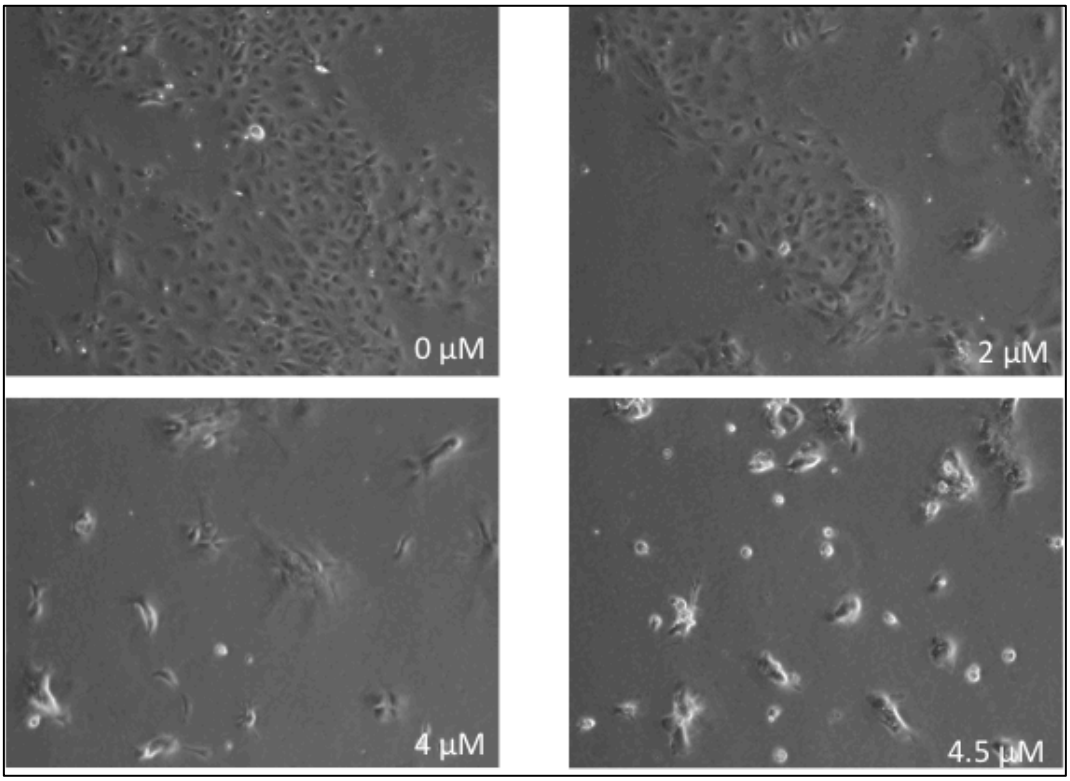

Figure 11. Phenotypic changes in differentiated keratinocytes with Methylstat drug treatment (differentiation occurred 24 hours post drug induction).

With higher concentrations of the Methylstat drug treatment, signs of apoptosis and decreased cellular proliferation were observed under the light microscope.

As we noticed the decrease in cellular growth and higher rates of cell death when high drug concentrations increased, we tested to see if Methylstat treatment caused high apoptosis when differentiation and Methylstat introduction occurred simultaneously. The data actually showed that there was little to no relative change between the negative control with no drug treatment and the highest concentration of Methylstat (4.5 μM).

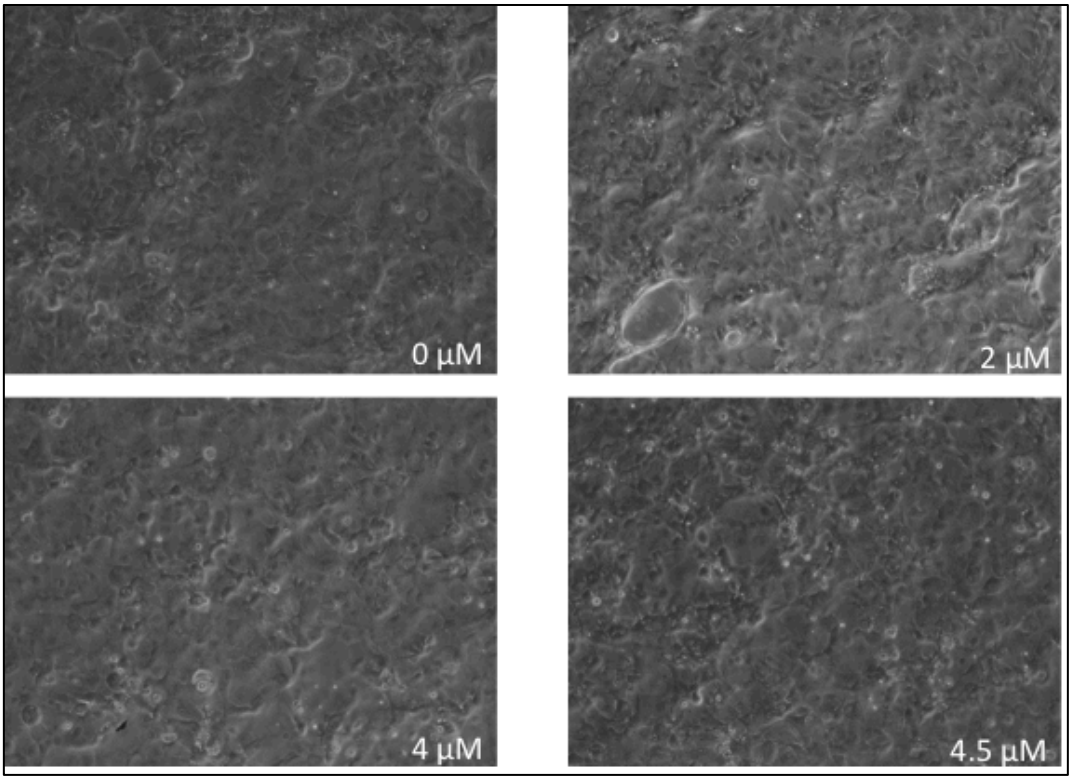

Figure 12. Phenotypic changes in differentiated keratinocytes with Methylstat drug treatment (differentiation occurred simultaneously with drug treatment).

With increasing concentrations of the Methylstat drug added, allowing the drug to interact with the keratinocytes with simultaneous induction of differentiation through high Calcium media, little to no morphological changes were observed under the light microscope.

Once we were able to identify a range of Methylstat dosage that did not completely kill the keratinocytes but still provided a viable phenotype, we tested Methylstat on squamous cell carcinoma cell lines. We treated Cal-27, SCC-4, and SCC-13 cells with 0 μM, 2 μM, and 4 μM of Methylstat. It is interesting to note that each strain of squamous cell carcinoma cells reacted slightly differently to Methylstat. Cal-27 cells did show higher rates of cellular death and decreased cellular growth after 48 hours; but already at 2 μM, rate changes in cellular growth/death were seen from the control and the effects on 4 μM were not as severe in Cal-27 cells as in normal keratinocytes.

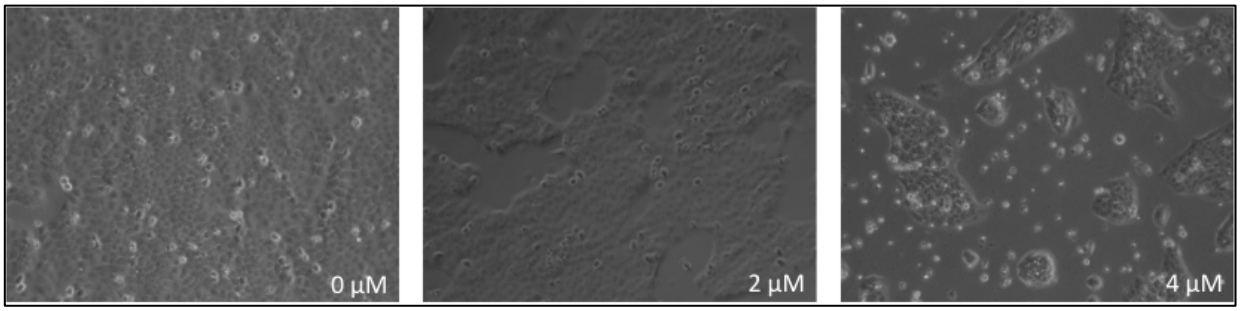

Figure 13. Cal-27 cells in Methylstat drug treatment.

Cal-27 cells demonstrated morphological and growth changes occurred at as low as 2 μM and more severe phenotypes persisted at 4 μM, where cell death seemed to be more frequently induced and less cellular proliferation appeared.

Next, SCC-13 cells were exposed to Methylstat after confluency was reached. We tested the cells under the same conditions as the Cal-27 cells, but the results more closely resembled keratinocytes with drug treatment. Ultimately, the control with no drug treatment and the 2 μM treated SCC-13 cells showed little to no difference, but the cells treated with 4 μM were not as propitious, having higher rates of cell death and less cellular growth.

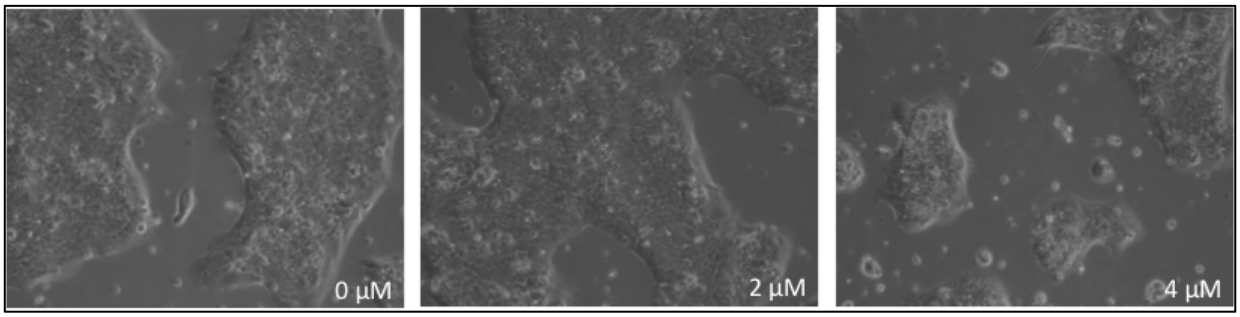

Figure 14. SCC-13 cells in Methylstat drug treatment.

SCC-13 cells demonstrate little to no change at 2 μM of drug induction constitutively throughout the plate. However, morphological changes were seen at 4 μM of drug treatment with lower rates of cellular growth and more apoptosis.

Lastly, SCC-4 cells were treated with Methylstat under the same conditions. Overall, SCC-4 cells portrayed a similar trend to Cal-27 cells with a gradual decrease in cells and growth from the control, 2 μM, and 4 μM; this demonstrates that these SCC cells have high susceptibility and sensitivity to Methylstat, even more than normal keratinocytes even though their morphology resembles proliferative cells the most.

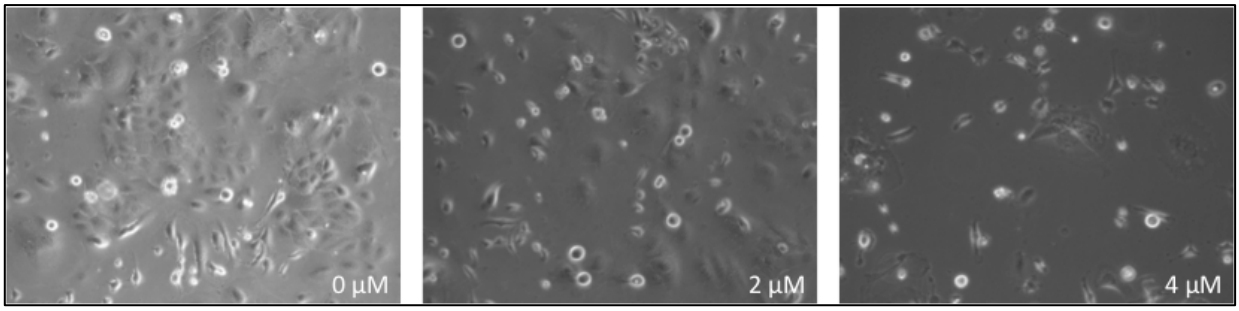

Figure 15. SCC-4 cells with Methylstat drug treatment.

SCC-4 cells demonstrated gradual decrease in cellular growth and higher rates of apoptosis already at 2 μM. Under the highest dose of 4 μM, significant cell death was observed throughout the cell culture plate.

Methylstat inhibits histone demethylation in keratinocytes

Although there is literature showing that Methylstat inhibits histone demethylation in tissue cell cultures, we needed to verify that the drug works in keratinocytes and not just human esophagus cancer (KYSE10) cells, as had been previously demonstrated. As such, we performed western blots to show that increasing the concentration of drug will show more inhibition of histone demethylation. β-Tubulin was used as a control and its expression was not affected with Methylstat drug treatment. Thus, using the same dosage compensation as before, the data shows that with increasing concentration of Methylstat, more signals appear with markers for H3K9me3 and H3K36me2. Ultimately, it can be inferred from this data that the Methylstat increases accumulation of histone methylation in a dosage response manner.

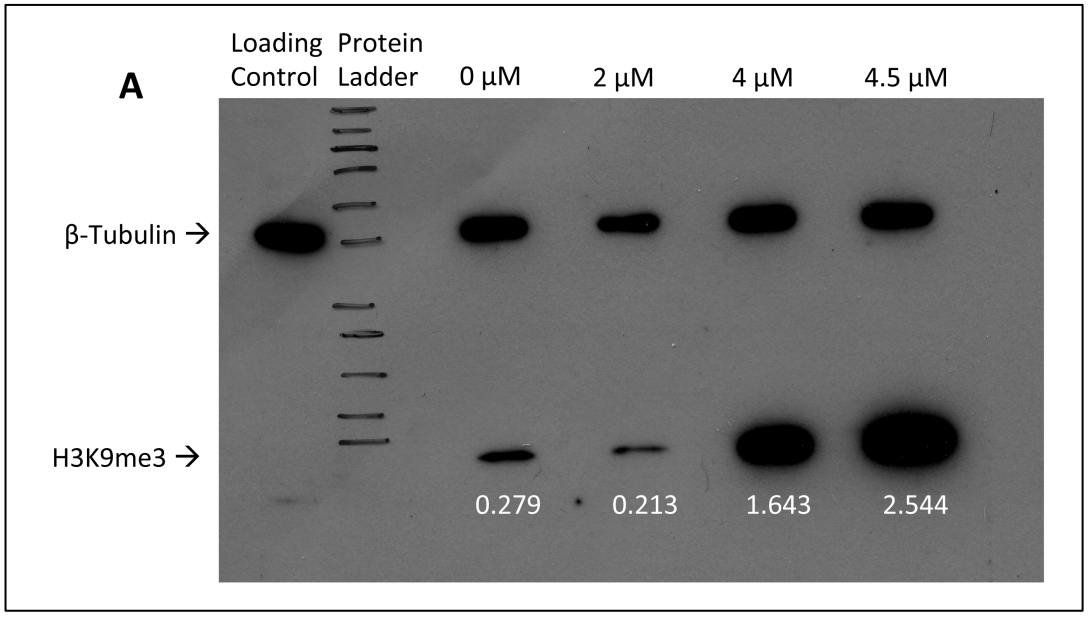

Figure 16. Western blot analysis of the effectiveness of the Methylstat drug on keratinocytes.

We used β-tubulin as the control for the experiment due to the high expression of β-tubulin in all cells. The results show that histone methylation accumulation occurred with higher concentrations of Methylstat. The white numbers below the bands represent the intensity ratio of the band respective to their β-tubulin control counterpart. **Figure 16A** illustrates β-tubulin did not change dramatically with higher treatments of the Methylstat drug, however the intensity of the H3K9me3 bands increased dramatically with higher dosages.

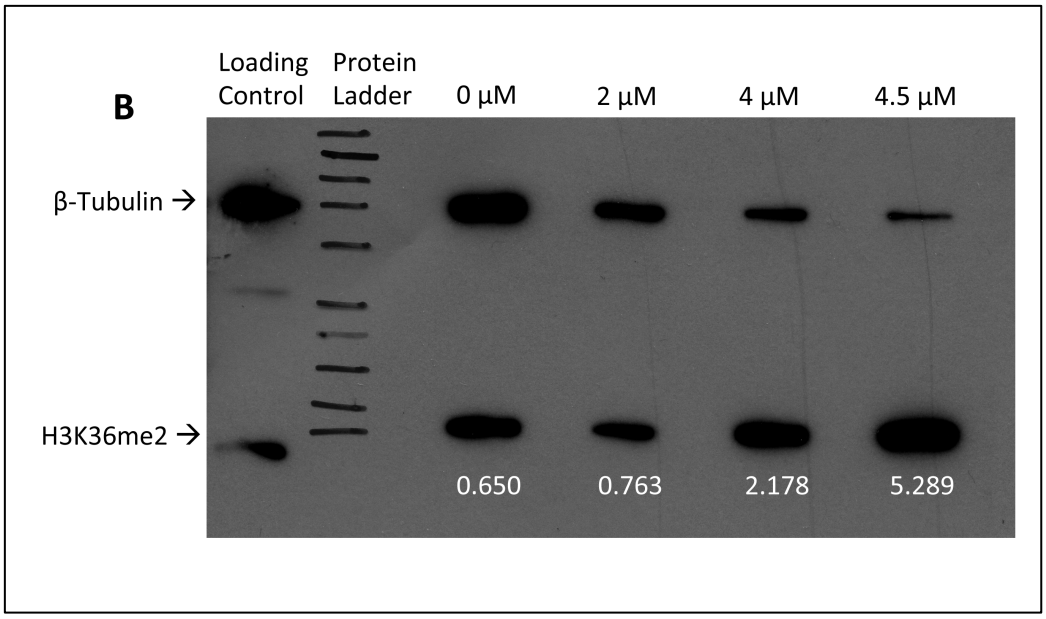

Figure 16. Western blot analysis of the effectiveness of the Methylstat drug on keratinocytes.

Figure 16B also illustrated the same results, although β-tubulin decreased as the Methylstat concentration increased, the intensity of the band increased for H3K36me2.

Methylstat immediately prevents cell cycle progression

Once we were able to confirm that treatment of keratinocytes with Methylstat inhibits histone demethylation, we performed cell cycle analysis on the keratinocytes to see where in the cell cycle the majority of the cells arrest. This allowed us to have a better profile of the impact of histone demethylation inhibition on skin cells. The data revealed that higher concentrations of Methylstat inhibit cell cycle progression in both keratinocytes and differentiated epithelial cells. We verified these results through both PI DNA staining and BrdU incorporation with Hoechst dye, since the BrdU labeling was more informative in the amount of cells that entered S phase in a given timeframe.

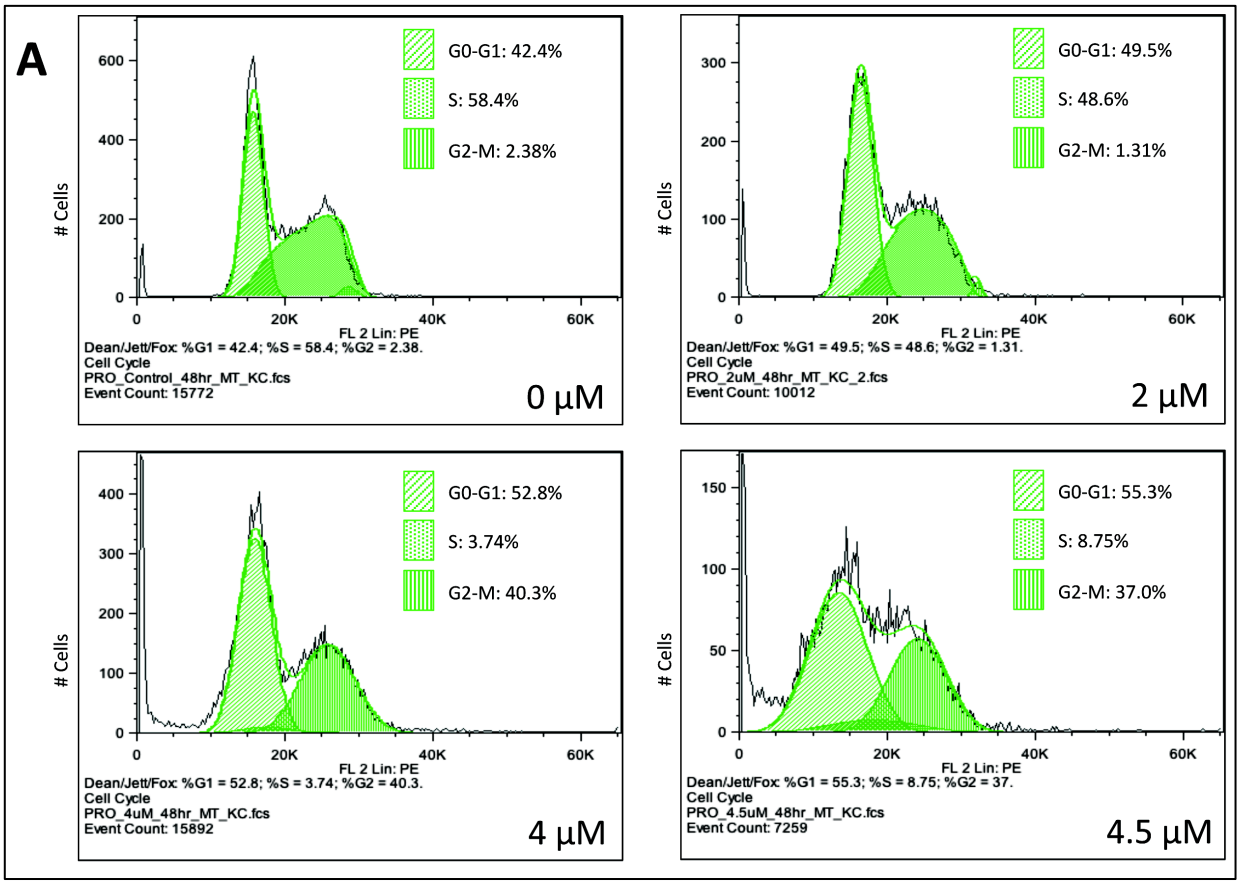

Figure 17. Cell cycle analysis for proliferative keratinocytes.

Figure 17A. This plot shows a comparison of the cell cycle data using PI to stain for DNA, using the Dean/Jett/Fox statistical analysis to give numerical values to each peak. The trend shows that the G0-G1 peak gets broader and more intense with higher concentrations of the Methylstat drug, as well as a decrease in S-phase cells with higher concentrations. Methylstat appears to impact the cell cycle progression of the proliferative cells.

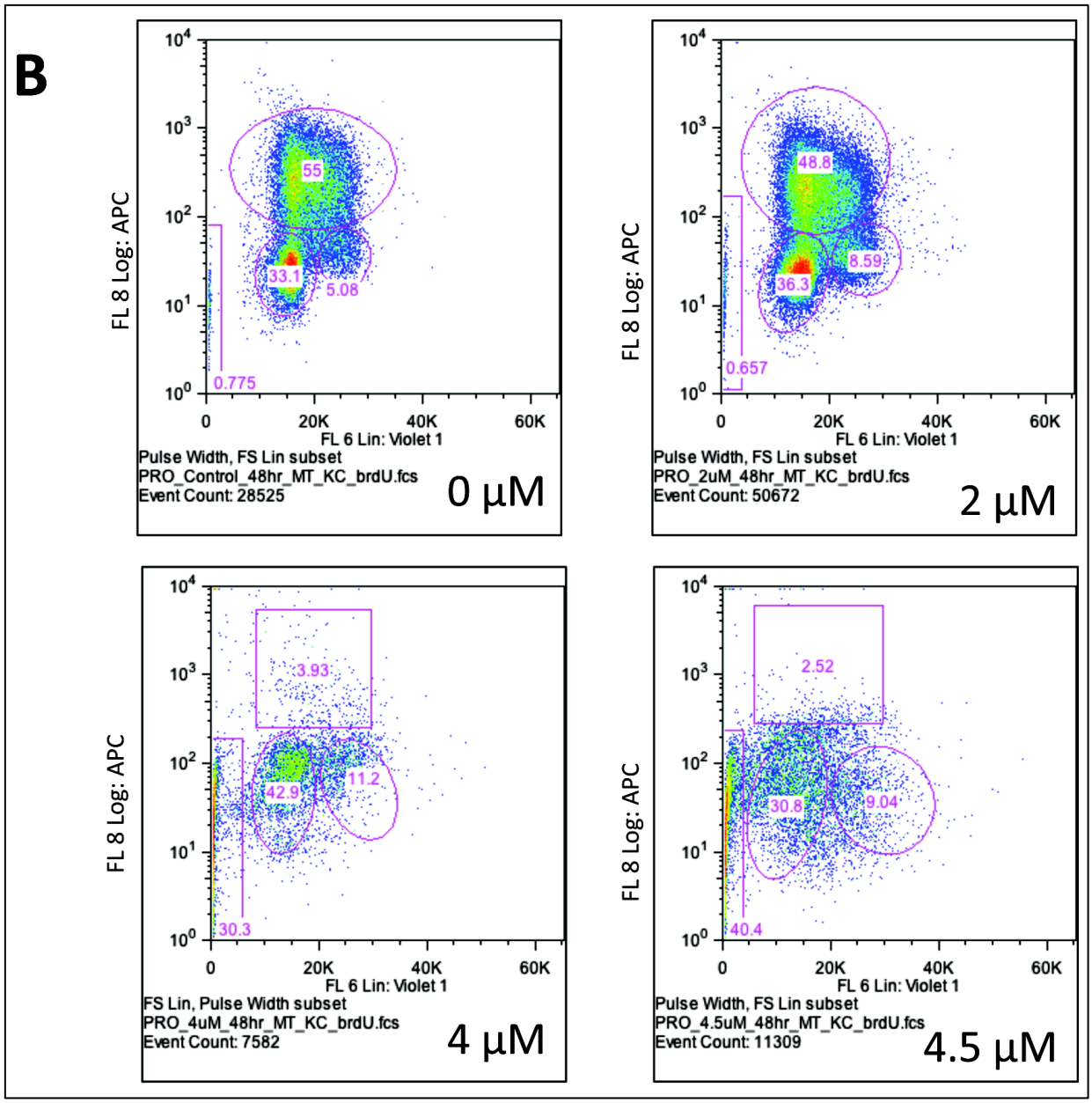

Figure 17. Cell cycle analysis for proliferative keratinocytes.

Figure 17B. This plot shows a comparison of cell cycle data with BrdU incorporation, which gives a more reliable quantitative data on the decrease in S-phase cells with higher concentrations of drug treatment. Also, this profile demonstrates how there is a spike in apoptotic cells in a dosage dependent manner, verifying the morphological results.

The DNA staining results for both the proliferative keratinocytes and differentiated epithelial cells show that higher concentrations of Methylstat cause higher rates of apoptosis, and

fewer cells are in the proliferative state. Additionally, the DNA staining results show that the linearity of the G0-G1 peak decreases with the increase of drug concentration in both proliferative and differentiated cells. The decrease in linearity signifies that the differentiated epithelial cells are behaving less like normal differentiated cells, such that the repression of histone demethylation affects their progression through the cell cycle. The BrdU incorporation cell cycle analysis data illustrates a decrease in S-phase cells as the drug concentration is increased, showing that a blockage is present prior to the S-phase so cells are exiting the cell cycle prematurely.

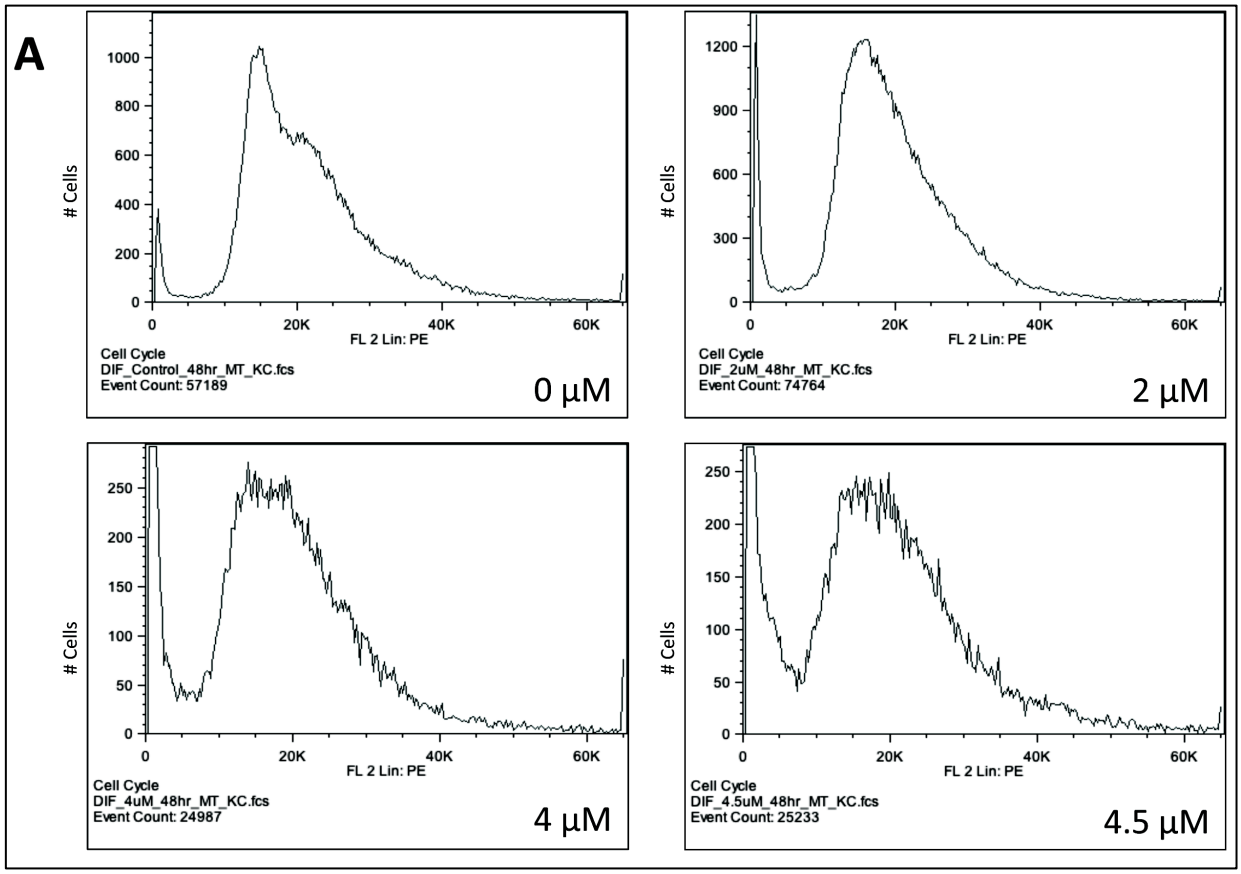

Figure 18. Cell cycle analysis data for differentiated epithelial cells.

Figure 18A. This plot shows a cell cycle profile of differentiated epithelial cells. No statistical analysis was used, because the algorithm curve could not fit the data. Again, the peak broadens with higher concentrations of drug treatment, but also the G2-M peak disappears with higher dosages.

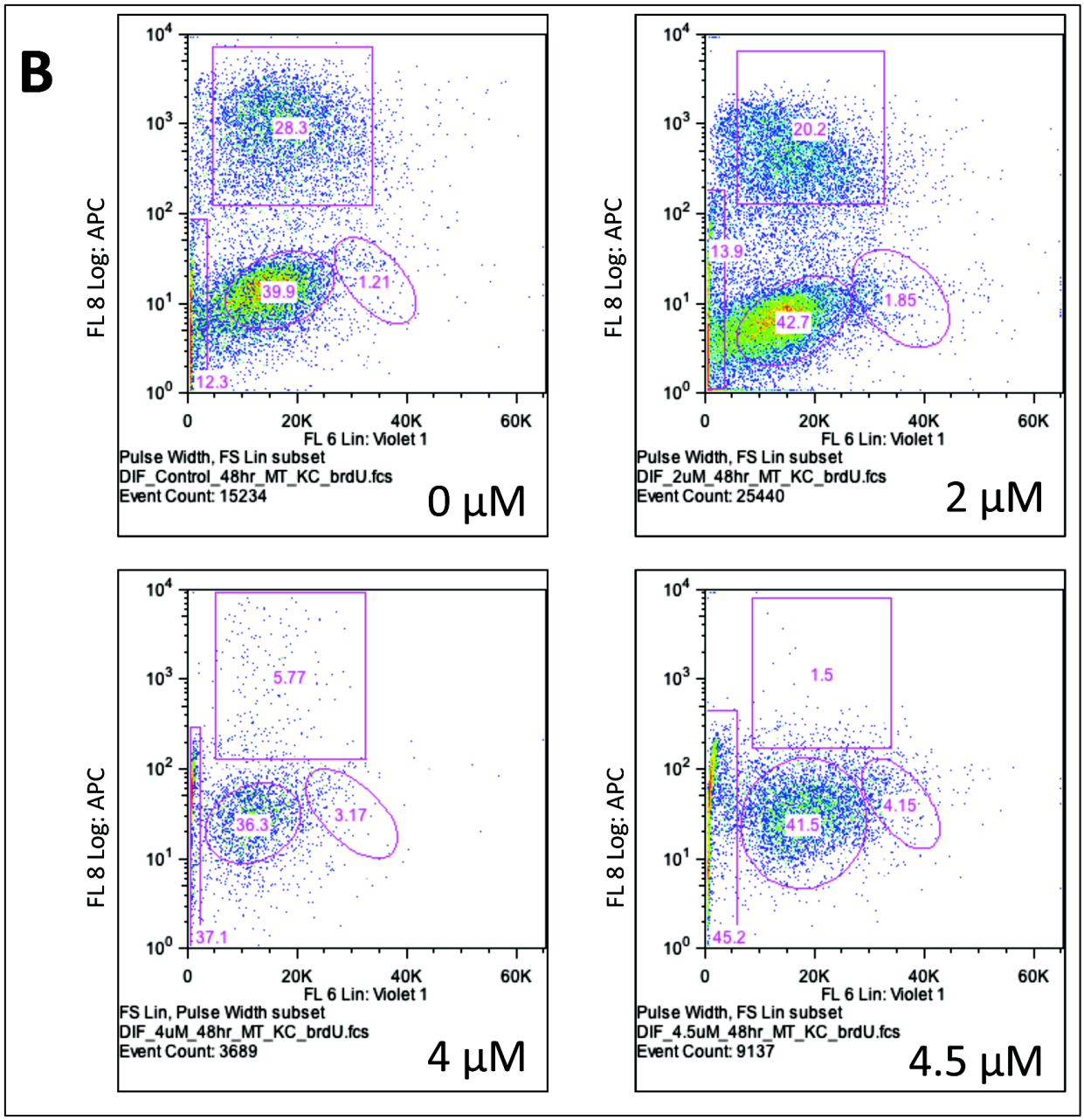

Figure 18. Cell cycle analysis data for differentiated epithelial cells.

Figure 18B. This plot shows a cell cycle profile with BrdU incorporation to quantify the amount of cells in the S-phase. Cells in the S-phase also decrease will higher dosages, but the amount of cells in the S phase is nearly two-fold less than in the proliferative cells, which is consistent with biological findings, since less cells undergo division once differentiated. In addition, the amount of apoptotic cells also increase in a dosage dependent manner, which is uniform with the results observed from the morphological assays.

Methylstat induces changes in differentiation of keratinocytes

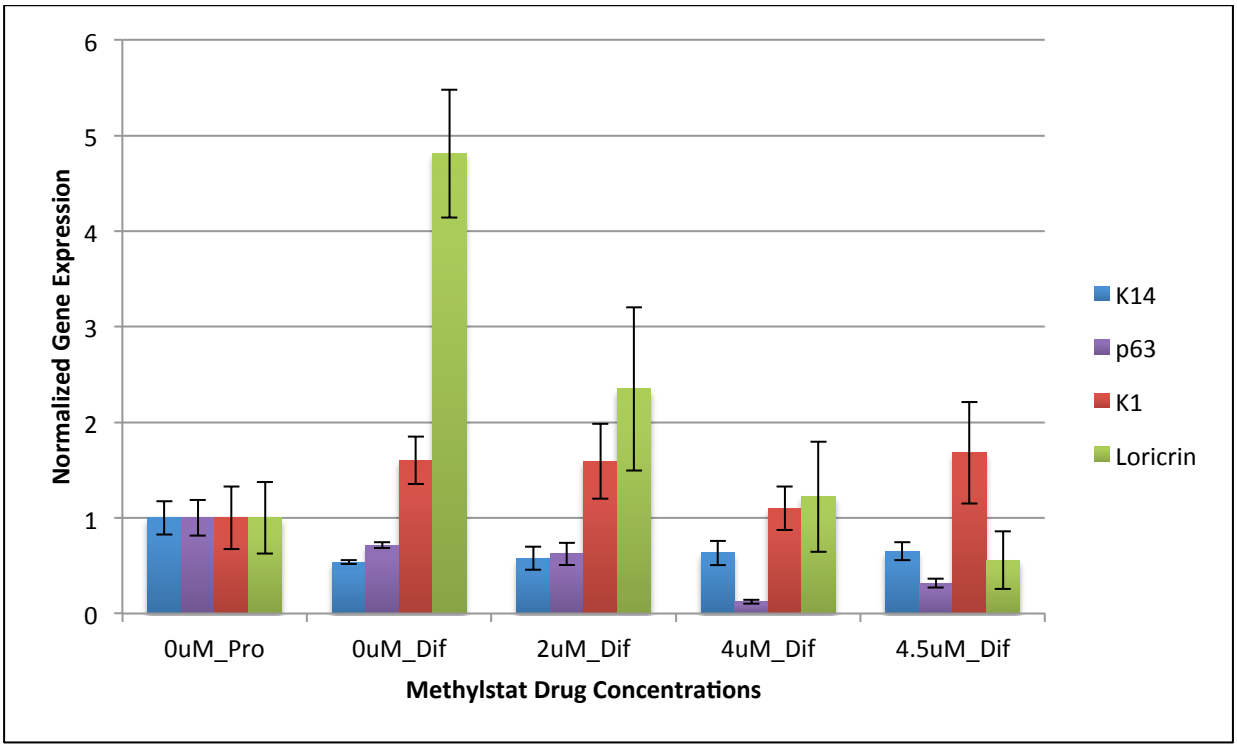

Figure 19. Normalized gene expression graph of differentiated epithelial cells with different concentrations of Methylstat treatment (mRNA samples).

Four different markers were used to test relative changes of gene expression with different concentrations of Methylstat drug: K1, K14, Loricrin, and p63. The gene expression levels of normal proliferative keratinocyte samples (0μM_Pro) were used to normalize the gene expression levels of the differentiated epithelial cells samples (Dif). Additionally, Actin and HPRT were used as internal controls and RT controls were also used to see if DNA was amplified during the production of cDNA.

After observing the morphologies of differentiated epithelial cells with Methylstat treatment, we performed a qPCR assay with specific markers to see if the gene expression levels change with different concentrations of Methylstat. Each marker showed different trends. K1 and K14 gene expression levels remained relatively similar across different drug concentrations. Loricrin demonstrated a dramatic reduction in gene expression with higher treatments of Methylstat and p63 illustrated a slight reduction as well. Loricrin is a late marker for

differentiation, and the dramatic decrease illustrates that Methylstat impacts differentiation pathways, since the sample of cells that were utilized in the experiment were keratinocytes that were treated with the drug simultaneous with induction of differentiation through the addition of high calcium media. The qPCR results also demonstrate a dosage response through the Loricrin marker, because an increase in drug concentration correlated with a decrease in Loricrin expression.

FoxN1-Cre marks differentiated cells in interfollicular epidermis

Given that the *in vitro* data using cell culture system gave us an idea of the impact of histone demethylation on the skin in proliferation and differentiation pathways, the use of an *in vivo* system allowed for further clarification. We needed to verify that FoxN1-Cre actually marks differentiated cells in the epithelium, by genotyping the mice to see if they possess the correct genotype and then staining the tissue with an X-gal antibody. The staining confirmed that Fox-N1 stained only the suprabasal layers on the interfollicular epidermis and differentiated cells in the hair follicle.

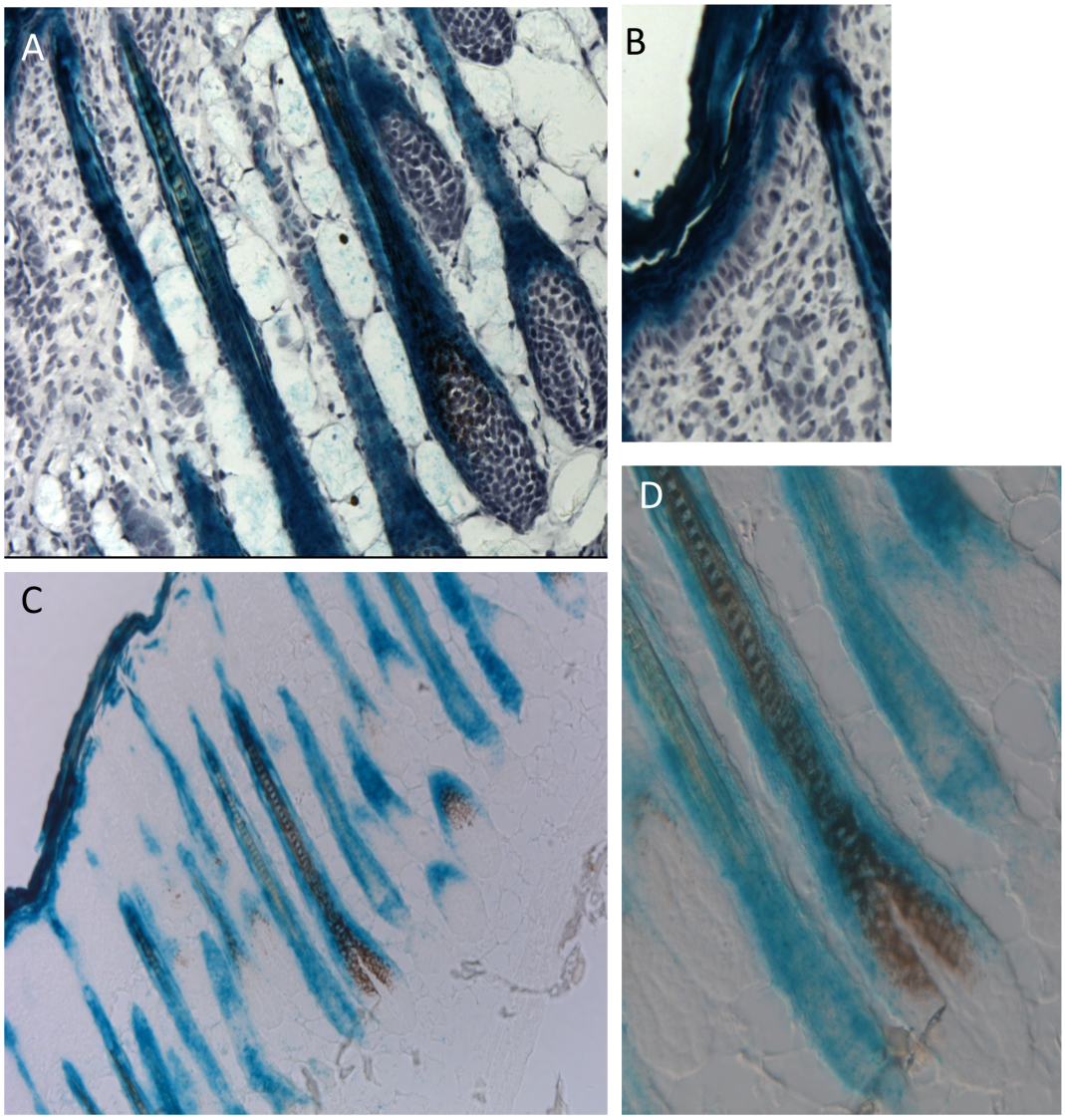

Figure 20. X-gal staining of FoxN1-Cre mice.

Figure 20A. X-gal stain, co-stained with hematoxylin of mouse hair follicle. **Figure 20B.** X-gal stain, co-stained with hematoxylin of mouse interfollicular epidermis. **Figures 20C & 20D.** X-gal stain by itself to show the effectiveness of FoxN1-Cre in marking differentiated cells in the mouse skin.

Discussion

The purpose of this project is to explore the functional role of histone demethylation in keratinocyte proliferation and differentiation, and to observe the effects of histone demethylation inhibition on human squamous cell carcinoma cells in order to compare the observed effects with those seen in normal keratinocytes through treatment with Methylstat.

Methylstat inhibits histone demethylation in keratinocytes

Treatment of keratinocytes with Methylstat showed that the drug is effective in inhibiting histone demethylation like the human esophagus cancer (KYSE10) cells described in literature. Although the conditions were not done completely the same, because culturing of different cells lines require different media, keratinocytes were treated with a Methylstat concentration up to 4.5 μM, because beyond this concentration killed majority of cells. In the original experiment by Luo et al. (2011), the KYSE10 cells were treated up to 10 μM with enough cell survival to preform a Western blot on histone methylation accumulation. It can be inferred that keratinocytes is more sensitive to the Methylstat or histone demethylation repression. This data shows that cells of different origin and cellular make-up can have varying sensitivities to the drug, allowing us to deduce that the function of histone demethylation can fluctuate for distinct tissues, so this process can be of more service for one cell than another.

Initially, to test the effectiveness of the drug in keratinocytes we began using the same dosage range as described in the literature. However, as described before, the results only portrayed high cellular death with little to no cell survival at the minimal dosage used in the article (5 μM). We performed a series of titrations to determine that around 4.5 μM; there was roughly 30-50% cell survival with significant histone methylation accumulation for both

H3K9me3 and H3K36me2 markers. Overall, these results show that Methylstat is highly effective in normal keratinocytes and has the potential to be (or is) a helpful tool in understanding the effects of histone demethylation on skin stem cell proliferation and differentiation processes.

Accumulation of histone methylation inhibits keratinocyte proliferation

Using keratinocytes treated with different concentrations of Methylstat, we found that there was significant decrease in cellular proliferation in a small range of concentrations. At as low as 4 μM, there was an immediate impact on the cell cycle, causing a large decline in cells in the S-phase. Not only did this occur in the 4 μM treated cells, but this was also a global occurrence throughout keratinocytes and terminally differentiated epithelial cells. Additionally, we saw a general trend in which fewer cells were present in S-phase as the concentration of Methylstat increased. The outlier in this trend were keratinocytes treated with 4.5 μM of the drug, which could be due to the fact that the high concentration of drug induced higher volumes of cellular death, skewing the overall profile. The BrdU profile demonstrated that the number of cells in the G2-M phase decreased along with the number of cells in the S-phase as the concentration of Methylstat increased. This indicates that cells are stuck in the cell cycle and unable to pass the G0 “check-point” to enter S-phase, which continues cellular proliferation. This is indicative that as there is more histone demethylation inhibition, fewer cells are able to proliferate and more cells are undergoing apoptosis. Thus, histone demethylation inhibition causes an obstruction in cell cycle progression of proliferative keratinocytes, which could mean that this process impacts proliferation pathways in keratinocytes.

When examining the morphological differences between keratinocytes and terminally differentiated epithelial cells, the effects were seen already after 24 hours of drug treatment for

keratinocytes and when drug treatment occurred before differentiation of cellular keratinocytes. The morphology of the cells changed; from all cells being initially rod-like, some cells retracted their cytoplasm and other cells elongated their cytoplasm in all directions but with little width, leading to a tentacle-like morphology. Overall, cells that were treated with Methylstat seemed very unhealthy compared to cells with no drug treatment, which proliferated quite rapidly. By 48 hours of Methylstat treatment, cells in the control group grew to near complete confluency. For the keratinocytes, cells with 2 μM Methylstat treatment had similar behavior as the control cells, because these cells also grew well. They had slightly more cells floating in the media, which is indicative of cellular death; however, the changes were mild. Yet, looking at cells treated in 4 μM and 4.5 μM of the Methylstat, there was widespread decrease in cellular proliferation. Not only did the cells look unhealthy, but also there were many cells floating in the dish and the number of cells still on the plate was minimal. These observations were quite universal with keratinocytes that were differentiated 24 hours after the drug treatment. In conclusion, the cell survival function that is usually present in proliferative cells was affected with histone demethylation inhibition.

On the other hand, keratinocytes that were differentiated simultaneously with drug treatment did not show morphological changes that differed from the control. Under the bright-field microscope, all the plates, no matter the amount of drug added (2, 4, or 4.5 μM) showed a normal differentiated phenotype. These results show that the repression of histone demethylation causes more dramatic effects on undifferentiated cells compared to differentiated cells according to the morphological differences that occurred when Methylstat is added before high calcium media is added to induce stratification of epithelial cells. Thus, once differentiation occurred in

keratinocytes, the cell survival function was not affected, but histone demethylation inhibition did impair the cell's ability to differentiate, so the differentiation program, itself, was affected.

Histone demethylation inhibition impacts differentiation pathways in keratinocytes

We further investigated these differentiated epithelial cells by analyzing the production of mRNA via qualitative PCR (qPCR). Cell cycle profiles were not collected for these cells that were differentiated concurrently with treatment of drug to induce histone demethylation inhibition because the profiles were so dissimilar to normal cell cycle profiles that the data was unable to be interpreted, which made the data unaccountable. With qPCR, we could test a wide variety of genes to get a general understanding of the global effects of histone demethylation on keratinocytes undergoing differentiation. We quantified both basal (K14) and suprabasal (K1 and Loricrin) markers, along with transcription factor p63. Overall, the results showed that the mRNA expression levels for K1 and K14 remained relatively unchanged with different dosages of Methylstat. As expected, the results showed that K1 levels increased once proliferative cells were differentiated and K14 levels would decline. However, between different dosages of Methylstat treatment, there was no clear trend seen in expression levels of K1 or K14. These results were expected, because during the differentiation process, there is an increase in K1 and a decrease in K14 expression. However, p63's expression decreased once the proliferating keratinocytes were differentiated. With increasing concentrations of Methylstat, the expression level of p63 waned with 4 or 4.5 μM. The decrease in p63 corresponding to the higher concentrations of Methylstat treatment reinforces the stipulation that histone demethylation regulation has an impact on differentiation and proliferation pathways in mammalian skin. Last but not least, the expression levels for Loricrin were highly unexpected. A significant dosage response was demonstrated in the qPCR results. We saw that from the transition between

proliferative keratinocytes to differentiated epithelial cells, there was a large increase in Loricrin expression. This is expected considering that Loricrin expression is high in the stratum corneum or during late terminal differentiation. However, with higher concentrations of Methylstat treatment, there was a substantial decline in expression. This data suggests that histone demethylation inhibition from Methylstat significantly impacts the differentiation pathway in keratinocytes. Largely, these results reinforce that histone demethylation inhibition causes a block in the cell cycle that leads to abnormal progression through proliferative pathways and; also the process of histone demethylation plays a role in the regulation of keratinocyte differentiation.

Inhibiting histone demethylation influences SCC cells more notably

Using different lines of human squamous cell carcinomas to test various dosages of Methylstat, we discovered that at lower concentrations, the inhibition induced more vivid phenotypes in the cancer cells in comparison with normal keratinocytes. At 2 μM, cell death and a reduced proliferation were already observed in Cal-27 and SCC-4 cells. This shows that not only is there a possibility that histone demethylation may play a role in epithelial cancer, but also implies that Methylstat is more effective on invasive cells than normal cells. This can potentially lead to a new generation of clinical treatments targeting epigenetic pathways for skin cancer.

FoxN1-Cre Expression Patterns

The results show that that FoxN1-Cre expression is contained within the suprabasal layers (terminally differentiated epithelial cells) and inner root sheath, which supports literature (Mizuguch et al., Molecular Therapy, 2000). In mouse skin, FoxN1 is mainly expressed in terminally differentiated cell lineages. This data suggests that the FoxN1-Cre model can be

helpful in testing the effects of histone demethylation inhibition in terminal differentiation of epithelial cells.

Limitations

In this project, the Dean/Jett/Fox algorithms were utilized to determine the percentage of cells in the G0/G1, S, and G2/M phase of the cell cycle profiles. Although a very helpful and useful tool, these algorithms were not successful at quantifying cells in different phases with differentiated epithelial cells, because the shape of the graph varied significantly. The atypical cell cycle profiles prevent these algorithms from providing any analysis, because the curvature of the graph is what allows the algorithm to provide a statistical analysis of each phase. A possible alternative is to provide additional markers that are distinctive to each phase, so the added dimensions can allow for more quantitative distinction between cells in different phase.

The qPCR results showed a dramatic increase in Loricrin but only a slight increase in K1 expression. This is indicative of the fact that that over the period of 48 hours, the keratinocytes underwent further terminal differentiation to the late stages, which seems like a very tight timeframe for such changes to occur. Therefore, changes in K1 expression from the data may not be as accurate, so duplication of experiment is required for verification of these results.

Recently, scientists have discovered that histone demethylases not only demethylate histones, but also other proteins in the cell (Ponnaluri et al., Biochemical and Biophysical Research Communications, 2009). Therefore, in interpreting the results in this project, it is important to take caution that it may not be completely attributed to the inhibition of histone demethylation.

Conclusion

Histone demethylation plays a wide variety of functional roles throughout the organism. It is known that histone demethylation plays a role in cell cycle control and regulation of differentiation pathways. Because of this, elucidating its role in maintenance and regulation of skin stem cell differentiation helps to provide a more complete picture of the complexity of cellular differentiation regulation within the skin. This project ultimately demonstrated that histone demethylation does play an integral role in skin cell proliferation and differentiation, providing preliminary results that can help determine critical functions of histone demethylases in skin. Explicitly, this project showed that inhibition of histone demethylation diminished the cell's survivability during proliferation and impaired the cell's differentiation program during differentiation with specific genes that are impacted during these processes. Furthermore, this project showed that squamous cell carcinoma cells are more sensitive to repression of histone demethylation, which is consistent with the fact that cancer cells are able to proliferate faster and more aggressively than normal cells.

Overall, performing a loss-of-function study of histone demethylases in the mouse is a difficult task due to the redundancy of enzyme genes, so the design of a competitive inhibitor and its use in this thesis study was the ideal system to study the role of histone demethylases in cellular function. Consequently, this project allowed for the exploration of unknown networks of stem cell regulation in the skin and the assessment the role of histone demethylase.

Larger Implications

Because histone demethylation plays a role in regulating cellular proliferation and differentiation, it is interesting to study this process in regard to cancer. Methylstat's potential for

inhibition of stem cell proliferation designates it as a potential clinical drug for tumor suppression. In fact, through the squamous cell carcinoma studies in this experiment, Cal-27 and SCC-4 lines demonstrated cellular death and decelerated cancer cell proliferation at as low as 2 μM, with more dramatic outcomes at 4 μM. Therefore, learning more about how this drug interacts with cancer cells in comparison with normal cells may allow this drug to become a novel example for the next generations of chemotherapy for cancer.

Future directions

The results in this project provide many directions for future studies. First of all, though this project provides an awareness of the genes that could be affected in the regulation of keratinocyte differentiation, it would be noteworthy to send the results for sequencing. The qPCR results are good preliminary data to demonstrate up- or down-regulation in certain genes in the proliferative or differentiated pathways; however, sequencing of these results can show if histone demethylation inhibition caused any changes in the genomic sequence of a particular gene.

Next, while this project looked at only a few genes involved in the regulation of differentiation, it did not look at the global effects of histone demethylation on keratinocytes. So, in addition to the qPCR results gained from this experiment, performing ChIP-sequencing on cells treated with various concentrations of Methylstat could show a more complete picture. This will provide valuable information with genes that have either enhanced or repressed transcription due to histone methylation accumulation. This will also provide valuable information about other genes that are affected during the differentiation processes in keratinocytes in response to histone demethylation inhibition. It would be exciting to see if there were trends as to which genes are more affected by histone demethylation inhibition compared with genes that are not regulated by

this process. Thus, studying the global effects of histone demethylation inhibition can further elucidate the specificity of the drug as well as genes that are particularly affected by histone demethylases. This will allow us to gain a better understanding of how Methylstat can potentially be used clinically as well as provide novel information on the degree of impact of histone demethylation regulation on gene expression and cell fate.

Third, this experiment only tested Methylstat in an *in vitro* study, which limits the results to only the cellular basis. However, with the use of the FoxN1-Cre transgenic mouse, the bioavailability of the drug to the skin, routes of administration, and effectiveness can be tested *in vivo*. This will expand on the implications made in this project and stipulate new information regarding the whole organism's response to Methylstat. Furthermore, it would be imperative to understand the role of histone demethylation in regulating the proliferation of cancer and whether the use of Methylstat can repress the spread of certain cancers. Abel et al. (2009) showed that squamous cell carcinoma could be induced in mice through chemical carcinogenesis. The induction of squamous cell carcinoma *in vivo* and then treatment with Methylstat could provide great information on the drug, such as bioavailability and where the drug mostly accumulates inside a body. These experiments can confirm that Methylstat decreases cancer proliferation and down-regulates genes that contribute to carcinogenesis, and could further suggest that Methylstat can be of great clinical use.

My learning experience

Through this project, I have been able to acquire some research experience and skills that I am able to carry on with me throughout my academic career. I learned that perseverance is an important attribute to have as a scientific researcher, because you frequently encounter failed

experiments. It is necessary to keep the mentality that you can't give up, because sometimes the solution may be as easy as going back to the basics.

My largest difficulty in this project encompassed the Western blot assays. I was unable to get any results for quite some time. After a few failed trials of conducting a Western blot under normal conditions utilized in the lab, I realized that I needed to optimize the protocol specific to histones, because its presence in the nucleus makes it slightly more difficult to isolate. After reading about the vendor's recommendations for the apparatus I was using, emailing post-doctorates at another university, and making some of my own changes referenced from literature I read regarding histones, I was finally able to get viable results. Just from this portion of this project, I learned that being persistent and not giving up can lead to a promising discovery.

Overall, the journey throughout this project has taught me a lot about myself and how science can be properly conducted. The molecular techniques helped me understand more about some biological systems and how to correctly perform certain experiments. Therefore, these experiences have helped augment my research experience by teaching me more about the underlying fundamentals of science and helping me appreciate the work that helped revolutionize the field of biology and bring about the discoveries we have today.

Methods and Materials

Keratinocyte cell culture

Keratinocytes were cultured using E low calcium media (containing 0.05 mM calcium chloride) and were split using 0.05% Trypsin-EDTA (incubation at 37 °C for ~5 min) when they reached ~90% confluence. Keratinocytes were differentiated using E high calcium media (containing 2.0 mM calcium chloride). All experiments were conducted with wild type keratinocytes at passage 11.

Keratinocyte isolation

Newborn mice were taken (~P0.5-P2) and the back skin was stripped from the mouse and put in 4% Dispase suspension at 4 °C overnight. After separation of the epidermis from the dermis layer, the epidermal layer was suspended in 0.05% Trypsin-EDTA for 10 min at 37 °C, filtered through a 70 μm filter and centrifuged for 5 min in 0.3 rcf at room temperature. Next, the newly acquired keratinocytes were suspended into E low calcium media on top of feeder cells (fibroblasts) for the first two passages.

Methylstat treatment in keratinocytes

Methylstat is stocked at 20 mM with a 1:1 ratio in DMSO. Cells were incubated at 37 °C for 48 hours with drug treatment prior to harvest. The keratinocytes were treated with 2, 4, and 4.5 μM of Methylstat and the negative control was treated with DMSO. The cells received new media also containing drug after 24 hours. Pictures of the morphological changes of the cells were taken at 0, 24, and 48 hours.

Methylstat treatment on differentiated skin epithelial cells for cell cycle analysis

Cells were plated on 10 cm plates, where cells were treated with 2, 4, and 4.5 μM of Methylstat and the negative control was treated with DMSO. Cells were incubated at 37 °C for 48 hours. Drug treatment started at 0 hour and new low calcium media with drug was added at 24 hours. High calcium media was added at 24 hour to induce differentiation in the keratinocytes. Whereas differentiation lasted 24 hours, the drug treatment lasted 48 hours, and cells were harvested at this time point. Pictures of the morphological change of the cells were taken at 0, 24, and 48 hours.

Methylstat treatment on differentiated skin epithelial cells for qPCR analysis

Cells were plated on a 6-well plate, where cells were treated with 2, 4, and 4.5 μM Methylstat and the negative control was treated with DMSO. Cells were incubated at 37 °C for 48 hours. Drug treatment and high calcium medium were introduced to the cells at 0 hour and new high calcium media with drug was added at 24 hours. Differentiation of the keratinocytes and drug treatment lasted for 48 hours, and cells were harvest at this time point. Pictures of the morphological change of the cells were taken at 0, 24, and 48 hours.

Squamous cell carcinoma (SCC) cell lines

Three different squamous cell carcinoma cell lines were used in this experiment: SCC-4, SCC-13, and Cal-27.

Squamous cell carcinoma cell culture

Human squamous cell carcinoma lines were cultured in DMEM:F-12 media supplemented with Penicillin-Streptomycin and FBS. Cells were split using 0.05% Trypsin-EDTA (incubation at 37 °C for ~5-8 min depending on strain) when they reached ~80%

confluency. SCC lines were not cultured on feeder cells so proliferation rates differ slightly from literature. Through the normal culturing conditions in this experiment, Cal-27, SCC-13, and SCC-4 decreased in proliferation rates.

Methylstat treatment on squamous cell carcinoma cells

Squamous cell carcinoma (SCC) cells were treated with 2 μM or 4 μM Methylstat from a stock of 20 mM (in 1:1 ratio of DMSO), plated on 6-well plates. The negative control was treated with DMSO. Cells were introduced to the drug at time 0 hour and the media was changed at 24 hours. Drug treatment on the SCC cells lasted for 48 hours and pictures were at 10x magnification under a light microscope of the morphological changes of the drug treated cells were taken at 0, 24, and 48 hours time-points.

Cell storage

All cells were aliquoted into 1 mL cryostat tubes and stored in the -80°C freezer in 95% E low medium and 5% DMSO.

Western Blot

Keratinocytes were washed in 1X PBS, and then incubated in 0.05% Trypsin-EDTA for 5 min. Next, the cells were harvested and centrifuged for 5 min at room temperature at 0.3 rcf. The cells were then suspended in EZ buffer (60 mM Tris-HCl at pH 6.8, 10% glycerol, and 2% SDS) for cell lysis. Subsequently, the total cell lysate was boiled at 100 °C for 10 min and then sonicated for 15 seconds with 5-second intervals in microfuge tubes. Samples were run on a 12% acrylamide/SDS-PAGE gel for 25 min at 70V and switched to 115V for 1.5 hours using the Bio-Rad Mini-PROTEAN Tetra Cell apparatus. The gel transfer was performed with 20% methanol overnight in 4 °C at 30V onto a PVDF membrane. Ponceau stain was performed immediately to

check for presence of protein. Blocking of the PVDF membrane was at RT for 1 hour. The antibodies used for this assay included β-Tubulin (αRb at 1:1000 from Ab-cam with 53 kDa) and H3K9me3 (αRb at 1:2000 from Ab-cam with 17 kDa). Film exposure was conducted using the Thermo-Scientific SuperSignal West Pico Chemiluminescent Substrate protocol.

Flow Cytometry

Propidium Iodide staining cell cycle analysis sample preparation

Keratinocytes (proliferative and differentiated) were washed in 1X PBS, and then incubated in 0.05% Trypsin-EDTA for 5-8 minutes at 37 °C. Proliferative cells were harvested subsequent to Trypsin incubation. Each plate of differentiated cells required incubation in 2 mL BD Cytofix/Cytoperm Buffer (commercially bought with BD Pharmingen APC BrdU Flow Kit) for 15 minutes prior to PBS wash and cells were taken off the dish with a scraper after trypsin incubation. Cells were centrifuged for 5 min at 0.4 rcf. Cells were re-suspended in 1X PBS and centrifuged again. Next, the excess PBS was aspirated until approximately 200 µL remained with the cell pellet. The cell pellet was re-suspended into the PBS solution. Afterwards, 1 mL of chilled 100% ethanol was added to the PBS-cell mixture drop by drop with constant movement to prevent cell precipitation. Cells were stored at -20 °C overnight. The following day, 1X PBS was added equal by volume and the mixture was centrifuged for 5 min at 0.4 rcf. After removing the supernatant, the cells were re-suspended in 500 µL DNA staining mixture (PBS, 100 µL/mL RNase A, and 40 µL/mL PI) for each sample.

BrdU/Hoechst dye cell cycle analysis sample preparation

Reagents from the BD Pharmingen APC BrdU kit were used in the following order. Sixty minutes prior to cell harvest, each plate of cells was pulsed with 10 µL of BrdU solution that was

added directlyto the tissue culture media at 37 °C. Next, the cells were washed with 1X PBS and 0.05% Trypsin-EDTA for 5-8 minutes (Note: differentiated cells were also incubated in 2 mL of BD Cytofix/Cytoperm Buffer for 15 minutes prior to PBS wash and trypsinization). Proliferative cells were harvested with a P1000 and differentiated cells were taken off the plate with a scraper. Each sample was centrifuged for 5 min at 0.4 rcf and the supernatant was aspirated, with the cell pellet remaining. The cell pellet was washed with 1X PBS and transferred to cell cycle flow tubes. All samples were then re-suspended in 100 µL BD Cytofix/Cytoperm Buffer for 15 minutes on ice and washed with 1X BD Perm/Wash Buffer. Cells were stored in staining buffer (PBS and 0.3% chelexed FBS) overnight in 4 °C. The following day, the cells were spun for 5 min at 0.45 rcf and the supernatant was removed. The cells were re-suspended in 100 µL BD Cytoperm Plus Buffer for 10 minutes on ice and then re-fixed in 100 µL of BD Cytofix/Cytoperm Buffer for 5 min on ice with cellular wash and spin in between each step. The cells were then treated with 300 µg/mL DNase for 1 hour in 37 °C (with wash and spin). Subsequently, cells were re-suspended in 50 µL of BD Perm/Wash Buffer with diluted fluorescent anti-BrdU antibodies (45 µg/mL) for 20 minutes at room temperature (with wash and spin). Finally, cells were suspended in 500 µL of DNA-staining mixture (1X Hoechst 33258 dye, 0.01% Triton-X, and PBS) for each sample.

Gating and Analysis

All samples were first gated using forward scatter vs. side scatter plots to separate cells from debris, and gated using forward scatter vs. pulse width plots to only gather data from single cell suspension. Next, cells were gated for event counts vs. PI fluorescence for cell cycle analyses using only DNA-staining and cells were gated for Hoechst dye fluorescence vs. BrdU

fluorescence for analyses using both methods. All gates were plotted and G0-G1, S, and G2-M phase gates were created to evaluate the cell cycle phase of each cell.

RNA Extraction and Isolation

Differentiated keratinocytes were washed with 1X PBS and then incubated in TRIzol (Sigma) for 10 minutes at room temperature. Next, the solution was collected into an RNase-free microfuge tube, where samples were frozen down to -80 °C. To continue the RNA extraction the protocol described by TRIzol reagent manual was used. RNA concentration was determined using a Nanodrop spectrophotometer and samples were diluted to the sample with the lowest concentration with dH_2O. cDNA was created as described in the miScript protocol. After acquiring cDNA, samples were stored at -20 °C.

Quanitative PCR

Real-time PCR quantification was performed using the Qiagen miScript system following the manufacturer's protocol. Cycles were run for40 cycles of 95 °C for 10 seconds, 60 °C for 10 seconds, and 72 °C for 30 seconds. HPRT and Actin were used as internal controls. qPCR results were measured using the Bio-Rad C1000 Thermal Cycler and analyzed with Bio-Rad's CFX384 Real-Time System software. Primer Sequences involved in this experiment were as follows:

HPRT	5'- TCAGTCAACGGGGGACATAAA 3'- GGGGCTGTACTGCTTAACCAG
Actin	5'- GCCAACCGTGAAAAGATGACCCAGATC 3'- TCGGTCAGGATCTTCATGAGGTAGTC
K1	5'- AGGAGAGAGACCTGCCATGA 3'- CTTTTGCCTTCTTGCTCCTG
K14	5'- CACGATACACCTGACTAGCTGGGTG 3'- CATCACCCACAGGCTAGCGCCAACT
Loricrin	5'- CGTCCCAACAGTATCAGTGCC 3'- TGGTCTGCTGAGAGGAGTAATAG
p63	5'- TTTGAAACTTCACGGTGTGC 3'- CCCAGATATGCTGGAAGACC

FoxN1^{ex9Cre}/R26R^{LacZ} staining

Mice were genotyped via PCR with appropriate primers, and the resulting amplified DNA was run on a 1% agarose gel. Mice containing the FoxN1^{ex9Cre}/R26R^{LacZ} cassette were sacrificed and the back-skin was peeled off and placed into O.C.T. (Tissue-Tek) and stored at -80 °C. The tissue was sectioned in a cross-sectional manner on the Cryostat and transferred onto glass slides for β-galactosidase staining. The tissue was fixed using LacZ Fix (1M Na Phosphate buffer pH 7.3 (PB), 37% Formaldehyde, 25% Glutaraldehyde, 0.2M EGTA, 1M $MgCl_2$) for 15-30 min and then washed with LacZ Wash (1M PB, $MgCl_2$, Deoxycholic Acid, NP40) 3x for 30 min each. Tissue was then stained using X-gal in a Ferri-Ferrocyanide solution for 24 hours. Each glass slide was subsequently co-stained with hemotoxylin for 30 seconds and mounted with a commercial fixative (i.e. Permount).

Acknowledgements

First, I would like to acknowledge all of the members of the Yi lab for their guidance, wisdom, and support throughout this project:

Rui Yi, Dongmei Wang, Xiying Fan, Jerome Lee, Kent Riemondy, Jie Zhang, Li Wang, Chris Bennett, Jaimee Hoefert, Lori Greiner, Emily Beans, Meaghan Flagg, Chris Ziegler, and Michelle Ferrall

I would also like to acknowledge all of my honor's thesis committee members:
Rui Yi, Johannes Rudolph and Sally Green

Lastly, I would like to acknowledge Victoria Hildreth, the Biological Science Initiative, UROP, and Greenhouse Scholars for giving me the opportunity to pursue my interest in research.

References

Abel, E., et al. (2009). "Multi-Stage Chemical Carcinogenesis in Mouse Skin: Fundamentals and Applications." *Nature Protocols* **4**(9): 1350–1362.

Alam, M., and Ratner, D. (2001). "Cutaneous Squamous-Cell Carcinoma." *The New England Journal of Medicine* **344**: 975-983.

Alonso, L., and Fuchs, E. (2003). "Stem Cells of the Skin Epithelium." *Proceedings of the National Academy of Sciences* **100**: 11830-11835.

Annunziato, A. (2008). "DNA Packaging: Nucleosomes and Chromatin." *Nature Education* **1**(1): Figure.

Avwioro, G. (2011). "Histochemical Uses Of Haematoxylin - A Review." *Journal of Physics and Chemistry of Solids* **1**: 24-34.

Barski, A., et al. (2007). "High-Resolution Profiling of Histone Methylations in the Human Genome." *Cell* **129**: 823-837.

Berger, S. (2002). "Histone Modifications in Transcriptional Regulation." *Current Opinion in Genetics & Development* **12**: 142-148.

Blanpain, C., and Fuchs, E. (2006). "Epidermal Stem Cells of the Skin." *Annual Review Cell Developmental Biology* **22**: 339–373 – Manuscript.

Frienkel, R., and Woodley, D. (2001). "The Biology of the Skin." *Pearl River, New York: The Parthenon Publishing Group Inc*. ppg 15-16.

Gioanni, J., et al. (1988). "Two New Human Tumor Cell Lines Derived from Squamous Cell Carcinomas of the Tongue: Establishment, Characterization and Response to Cytotoxic Treatment." *European Journal of Cancer and Clinical Oncology* **24**(9): 1445–1455.

Goldman, G. (1998). "Squamous Cell Cancer: A Practical Approach." *Seminars in Cutaneous Medicine and Surgery* **17**(2): 80-95.

He, Y., et al. (2012). "Targeting Protein Lysine Methylation and Demethylation in Cancers." *Acta Biochimica et Biophysica Sinica* **44**(1): 70–79.

Hennings, H., et al. (1980). "Calcium Regulation of Growth and Differentiation of Mouse Epidermal Cells in Culture." *Cell* **19**(1): 245-254.

Horwitz, J., et al. (1964). "Substrates for Cytochemical Demonstration of Enzyme Activity. Some Substituted 3-indolyl-β-D-glycopyranosides." *Journal of Medicinal Chemistry* **7**: 574-575.

Huber, M., et al. (1994). "Abnormal Keratin 1 and 10 Cytoskeleton in Cultured Keratinocytes from Epidermolytic Hyperkeratosis Caused by Keratin 10 Mutations." *Journal of Investigative Dermatology* **102**: 691-694.

Janes, S., et al. (2004). "Transient Activation of FOXN1 in Keratinocytes Induces a Transcriptional Program that Promotes Terminal Differentiation: Contrasting Roles of FOXN1 and Akt." *Journal of Cell Science* **117**(18): 4157-4168.

Klose, R., et al. (2006). "JmjC-Domain Containing Proteins and Histone Demethylation." *Nature Reviews Genetics* **7**: 715-727.

Klose, R., and Zhang, Y. (2007). "Regulation of Histone Methylation by Demethylimination and Demethylation." *Nature Reviews* **8**: 307-318.

Kouzarides, T. (2002). "Histone Methylation in Transcriptional Control." *Current Opinion in Genetics & Development* **12**(2): 198-209.

Lewis, J., et al. (1994). "Cadherin Function Is Required for Human Keratinocytes to Assemble Desmosomes and Stratify in Response to Calcium." *The Journal of Investigative Dermatology* **102**: 870-877.

Li, X., and Zhao, X. (2008). "Epigenetic Regulation of Mammalian Stem Cells." *Stem Cells and Development* **17**:1043–1052.

Lu, Y., et al. (2009). "Lung Cancer-Associated JmjC Domain Protein MDIG Suppresses Formation of Tri-methyl Lysine 9 of Histone H3 - Report." *Cell Cycle* **8**(13): 2101-2109.

Luo, X., et al. (2011). "A Selective Inhibitor and Probe of the Cellular Functions of Jumonji C Domain-Containing Histone Demethylases." *Journal of the American Chemical Society* **133**: 9451–9456.

Mizuguchi, H., et al. (2000). "IRES-Dependent Second Gene Expression Is Significantly Lower Than Cap-Dependent First Gene Expression in a Bicistronic Vector." *Molecular Therapy* **1**: 376–382.

Peterson, C., and Laniel, M. (2004). "Histones and Histone Modifications." *Current Biology* **14**(14): 546-551.

Ponnaluri, V., et al. (2009). "Identification of Non-Histone Substrates for JMJD2A–C Histone Demethylases." *Biochemical and Biophysical Research Communications* **390**(2): 280–284.

Sanchez, R., and Zhou, M. (2009). "The Role of Human Bromodomains in Chromatin Biology and Gene Transcription." *Current Opinion Drug Discovery Development* **2**(5): 659–665.

Shi, Y., and Whetstine, J. (2007). "Dynamic Regulation of Histone Lysine Methylation by Demethylases." *Molecular Cell Review* **25**: 1-14.

Tsukada, Y., et al. (2006). "Histone Demethylation by a Family of JmjC Domain-Containing Proteins." *Nature* **439**: 811-816.

Truong, A., et al. (2006). "p63 Regulates Proliferation and Differentiation of Developmentally Mature Keratinocytes." *Genes & Development* **20**: 3185-3197.

Varier, R., and Timmers, H. (2011). "Histone Lysine Methylation and Demethylation Pathways in Cancer." *Biochimica et Biophysica Acta* **1815**: 75–89.

Wang, L., et al. (2013). "Genome-Wide Maps of Polyadenylation Reveal Dynamic mRNA 3'-end Formation in Mammalian Cell Lineages." *RNA* **19**: 413-425.

Yang, A., et al. (1999). "p63 is Essential for Regenerative Proliferation in Limb, Craniofacial and Epithelial Development." *Nature: letters to Nature* **398**: 714-718.

Yi, R., and Fuchs, E. (2010). "MicroRNA-Mediated Control in the Skin." *Cell Death and Differentiation* **17**(2): 229–235.

Supplementary Information

Experiment Timeline

Figure 10. Phenotypic changes in keratinocytes with Methylstat drug treatment.

Day 1 (0 hr)	• Added Methylstat drug into new media • Aspirated out old media and washed cells with 1X PBS • Added media + drug into cell plates
Day 2 (24 hr)	• Added Methylstat drug into new media • Aspirated out old media and washed cells with 1X PBS • Added media + drug into cell plates
Day 3 (48 hr)	• Harvest cells

Figure 11. Phenotypic changes in differentiated keratinocytes with Methylstat drug treatment (differentiation occurred 24 hours post drug induction).

Day 1 (0 hr)	• Added Methylstat drug into new media • Aspirated out old media and washed cells with 1X PBS • Added media + drug into cell plates
Day 2 (24 hr)	• Added Methylstat drug into new high calcium media • Aspirated out old media and washed cells with 1X PBS • Added (high calcium) media + drug into cell plates
Day 3 (48 hr)	• Harvest cells

Figure 12. Phenotypic changes in differentiated keratinocytes with Methylstat drug treatment (differentiation occurred simultaneously with drug treatment).

Day 1 (0 hr)	• Added Methylstat drug into new high calcium media • Aspirated out old media and washed cells with 1X PBS • Added (high calcium) media + drug into cell plates
Day 2 (24 hr)	• Added Methylstat drug into new high calcium media • Aspirated out old media and washed cells with 1X PBS • Added (high calcium) media + drug into cell plates
Day 3 (48 hr)	• Harvest cells

Figure 13/14/15: Squamous cell carcinoma lines (Cal-27, SCC-13, SCC-4) treated with Methylstat drug.

Day 1 (0 hr)	• Added Methylstat drug into DMEM:F-12 media • Aspirated out old media and washed cells with 1X PBS • Added DMEM: F-12 media + drug into cell plates
Day 2 (24 hr)	• Added Methylstat drug into DMEM:F-12 media • Aspirated out old media and washed cells with 1X PBS • Added DMEM: F-12 media + drug into cell plates
Day 3 (48 hr)	• Harvest cells

Gating for Cell Cycle Profiles

Gating for PI DNA-staining

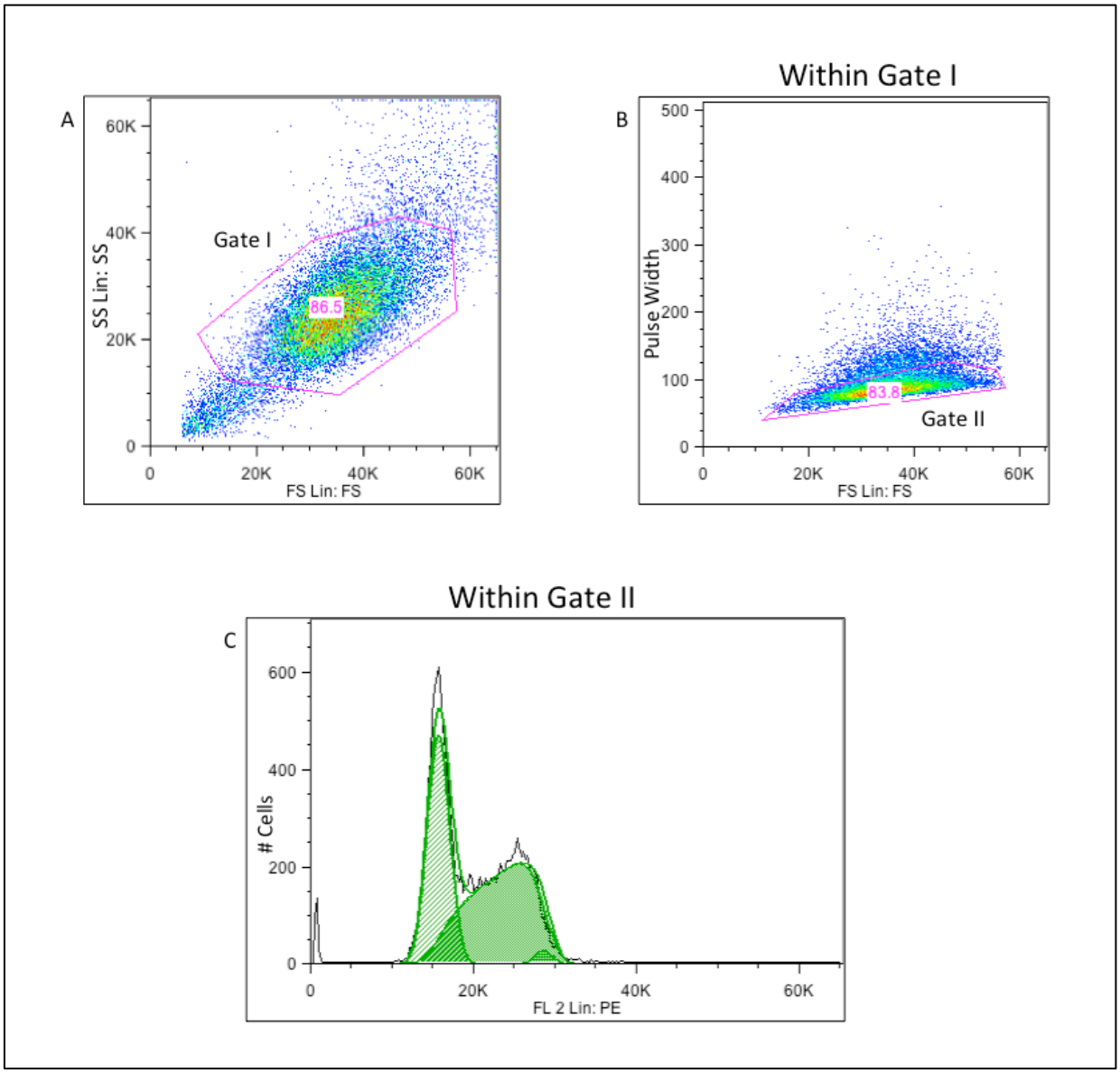

Supplementary Figure 1. PI DNA-staining cell cycle analysis gating.

A. Forward scatter vs. side scatter to select for cells and exclude debris. **B.** Forward scatter vs. pulse width to select for single cell suspension and not doublets. **C.** PE vs. number of cells to have final cell cycle analysis plot based on PI DNA staining.

Gating for BrdU and Hoechst dye staining

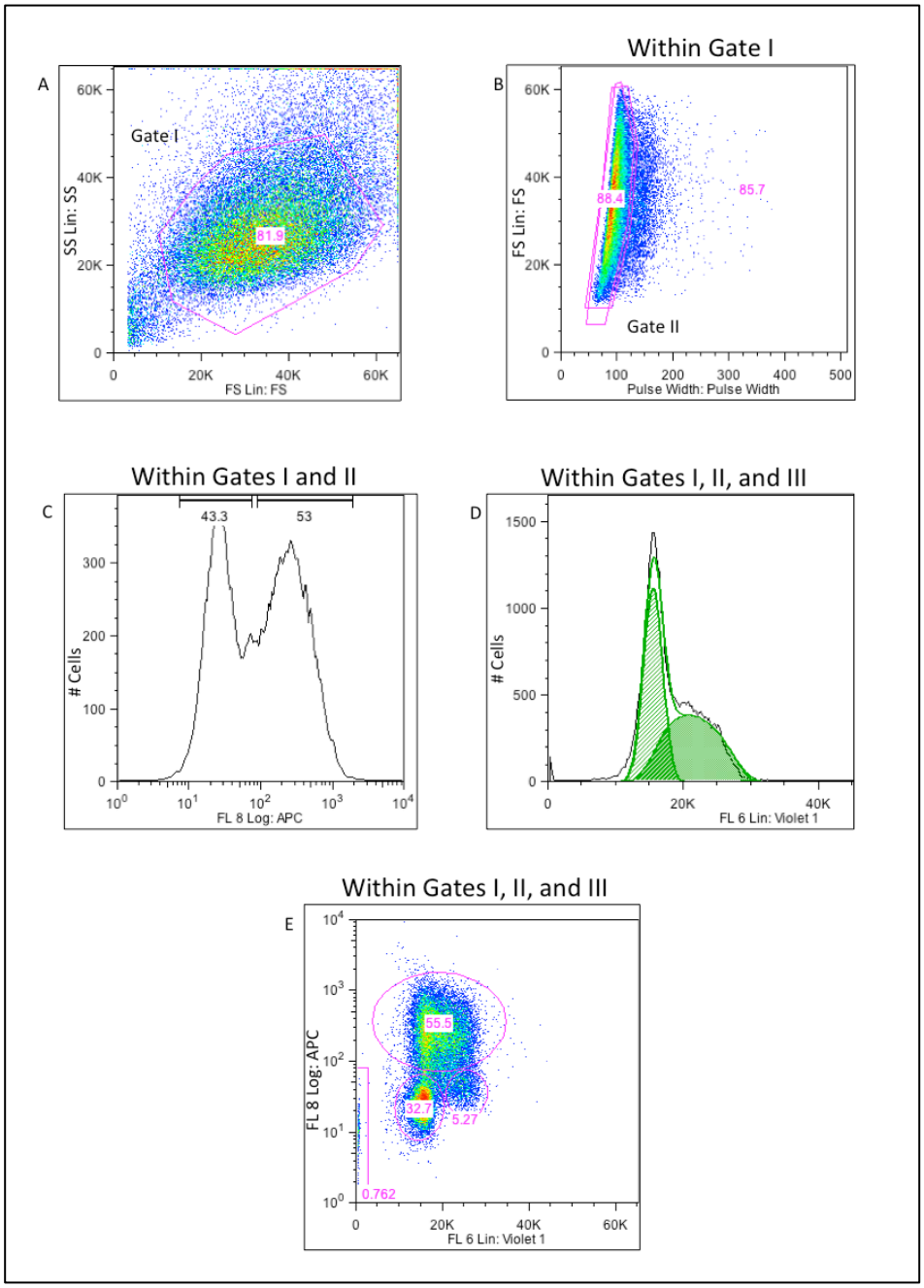

Supplementary Figure 2. BrdU cell cycle analysis gating.

A. Forward scatter vs. side scatter to select for cells and exclude debris. **B.** Forward scatter vs. pulse width to select for single cell suspension and not doublets. **C.** APC vs. number of cells to visualize the distribution of cells with BrdU incorporation into their genome. **D.** Violet 1 vs. number of cells to see the cell cycle profile based on Hoechst dye DNA-staining. **E.** Overall BrdU cell cycle analysis plot with gates applied.

qPCR Amplification

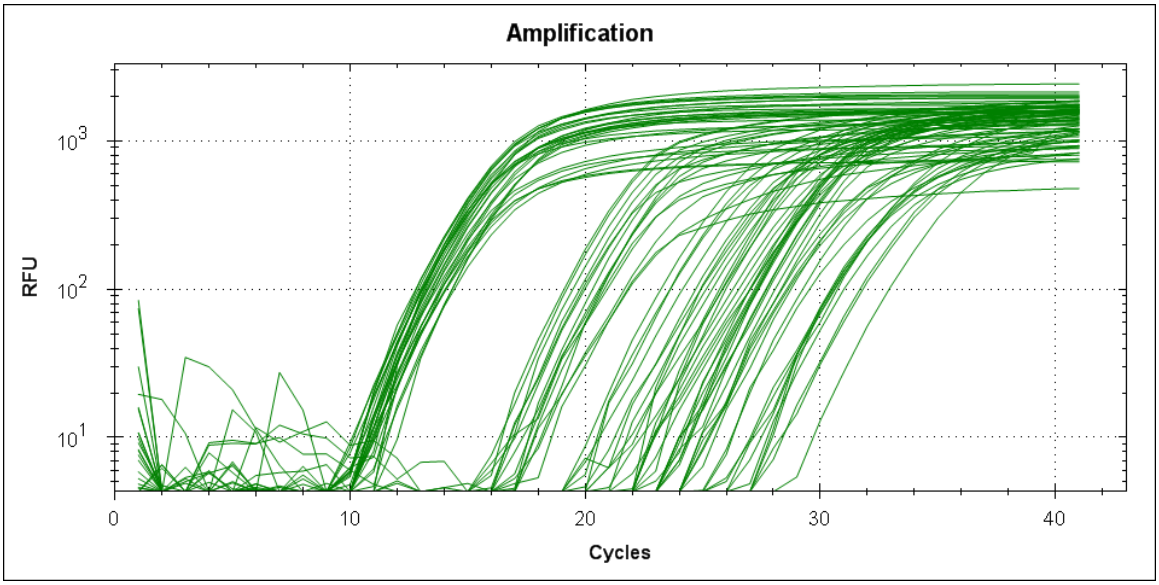

Supplementary Figure 3. Application graph of samples for qPCR.

This graph illustrates the curve of gene amplification of different samples. This graph is primarily used to determine the quality of the sample during amplification and whether something has gone wrong during the measure of SYBR Green activity. It is important to consider the threshold of the sample and the slope.

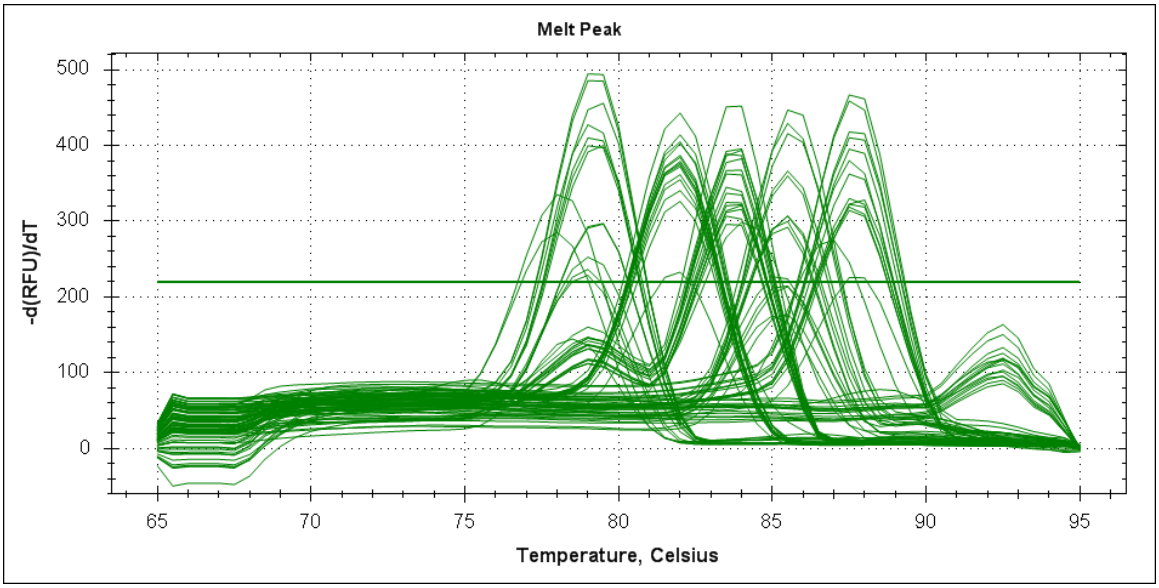

Supplementary Figure 4. Melt Peak graph of samples for qPCR.

This graph illustrates melting peaks of each sample relative to their primers. This graph is primarily used to see the quality of the primer used to amplify the gene of target.

Embedding and Sectioning

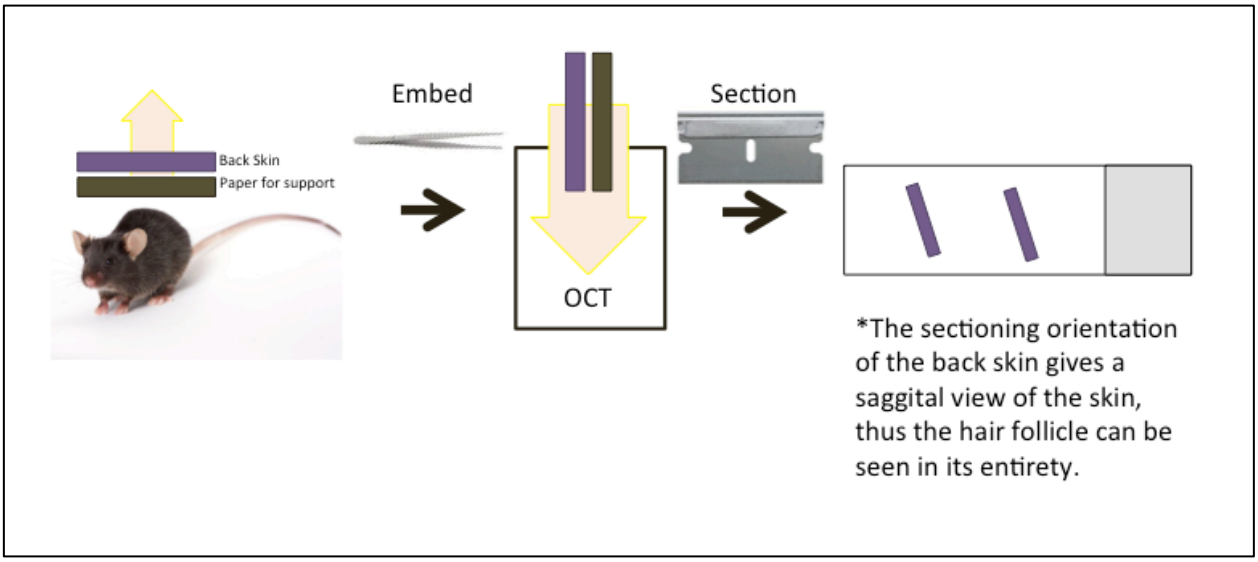

Supplementary Figure 5. Diagram representation of embedding and sectioning of mouse back skin